การสังเคราะห์แอลพีจีโดยตรงจากแก๊สสังเคราะห์บนตัวเร่งปฏิกิริยาลูกผสมของ
คอปเปอร์ซิงก์ออกไซด์และเส้นใยซิลิกาเคลือบด้วย ZSM-5

นายวิทวัส รัตนถาวร

วิทยานิพนธ์นี้เป็นส่วนหนึ่งของการศึกษาตามหลักสูตรปริญญาวิทยาศาสตรดุษฎีบัณฑิต
สาขาวิชาเคมีเทคนิค ภาควิชาเคมีเทคนิค
คณะวิทยาศาสตร์ จุฬาลงกรณ์มหาวิทยาลัย
ปีการศึกษา 2557

DIRECT SYNTHESIS OF LPG FROM SYNGAS OVER HYBRID CATALYST OF Cu/ZnO AND

SILICA FIBER COATED WITH ZSM-5

Mr. Wittawat Ratanathavorn

A Dissertation Submitted in Partial Fulfillment of the Requirements

for the Degree of Doctor of Philosophy Program in Chemical Technology

Department of Chemical Technology

Faculty of Science

Chulalongkorn University

Academic Year 2014

Thesis Title	DIRECT SYNTHESIS OF LPG FROM SYNGAS OVER HYBRID CATALYST OF Cu/ZnO AND SILICA FIBER COATED WITH ZSM-5
By	Mr. Wittawat Ratanathavorn
Field of Study	Chemical Technology
Thesis Advisor	Assistant Professor Dr. Prasert Reubroycharoen, D.Eng.

Accepted by the Faculty of Science, Chulalongkorn University in Partial Fulfillment of the Requirements for the Doctoral Degree

                                                              Dean of the Faculty of Science

(Professor Dr. Supot Hannongbua, Ph.D.)

THESIS COMMITTEE

                                                              Chairman

(Associate Professor Dr. Kejvalee Pruksathorn, Dr.de L'INPT)

                                                              Thesis Advisor

(Assistant Professor Dr. Prasert Reubroycharoen, D.Eng.)

                                                              Examiner

(Professor Dr. Tharapong Vitidsant, Dr.de L'INPT)

                                                              Examiner

(Associate Professor Dr. Chawalit Ngamcharussrivichai, Ph.D.)

                                                              External Examiner

(Assistant Professor Dr. Chanatip Samart, D.Eng.)

วิทวัส รัตนถาวร : การสังเคราะห์แอลพีจีโดยตรงจากแก๊สสังเคราะห์บนตัวเร่งปฏิกิริยาลูกผสมของคอปเปอร์ซิงก์ออกไซด์และเส้นใยซิลิกาเคลือบด้วย ZSM-5 (DIRECT SYNTHESIS OF LPG FROM SYNGAS OVER HYBRID CATALYST OF Cu/ZnO AND SILICA FIBER COATED WITH ZSM-5) อ.ที่ปรึกษาวิทยานิพนธ์หลัก: ผศ. ดร. ประเสริฐ เรียบร้อยเจริญ, 90 หน้า.

การสังเคราะห์แอลพีจีสามารถดำเนินการโดยการใช้ตัวเร่งปฏิกิริยาลูกผสมของคอปเปอร์/ซิงก์ออกไซด์-เซอร์โคเนีย-อะลูมินาและเส้นใยซิลิกาเคลือบด้วย ZSM-5 ตัวเร่งปฏิกิริยาสังเคราะห์เมทานอลที่เป็นคอปเปอร์/ซิงก์ออกไซด์-เซอร์โคเนีย-อะลูมินาถูกเตรียมด้วยวิธีการตกตะกอนร่วมและเส้นใยซิลิกาเคลือบด้วย ZSM-5 ถูกเตรียมด้วยวิธีโซลเจลและโดยกระบวนการอิเล็กโทรสปินนิงตามด้วยกระบวนการไฮโดรเทอร์มอล เตตระเอทิลออโธซิลิเกตและอะลูมิเนียมไนเตรตถูกใช้เป็นแหล่งของซิลิกอนและอะลูมิเนียมตามลำดับและใช้เตตระโพรพิลแอมโมเนียมไฮดรอกไซด์เป็นเบสอินทรีย์ เส้ยใยซิลิกาเคลือบด้วย ZSM-5 ถูกสังเคราะห์ที่เวลาในการเกิดผลึกต่างๆ (24 48 72 และ 120 ชั่วโมง) ที่ค่ากรด-เบสของสารละลายในช่วงต่างๆ (8 9 และ 10) และสัดส่วนโดยซิลิกอนต่ออะลูมิเนียม Si/Al (20 40 และ 60) ที่ภาวะเหมาะสมในการเตรียม ZSM-5 บนเส้นใยซิลิกา คือ การเตรียมโดยใช้เวลาในการเกิดผลึก 48 ชั่วโมง อุณหภูมิ 180 องศาเซลเซียส ที่ค่ากรด-เบสเท่ากับ 9 โดยมีพื้นที่ผิวเท่ากับ 273 ตารางเมตร/กรัม เส้ยใยซิลิกาเคลือบด้วย ZSM-5 มีข้อได้เปรียบมากกว่าตัวเร่งปฏิกิริยาในรูปแบบอื่นๆ เช่น แบบผงและแบบเม็ด โดยมีความยืดหยุ่นสามารถจัดเรียงตัวเข้าไปในช่องการไหลได้อย่างดี ความสามารถในการเร่งปฏิกิริยาของเส้นใยซิลิกาเคลือบด้วย ZSM-5 ถูกทดสอบโดยการผสมกับตัวเร่งปฏิกิริยาคอปเปอร์/ซิงก์ออกไซด์-เซอร์โคเนีย-อะลูมินาในเครื่องปฏิกรณ์แบบเบดนิ่งสำหรับกระบวนการสังเคราะแอลพีจีจากแก๊สสังเคราะห์และดำเนินการเปรียบเทียบกับตัวเร่งปฏิกิริยารูปแบบผงที่เป็นรูปแบบดั้งเดิม ค่าร้อยละการเปลี่ยนคาร์บอนมอนอกไซด์ที่สูงที่สุดได้จากการใช้ตัวเร่งปฏิกิริยาลูกผสมของคอปเปอร์/ซิงก์ออกไซด์-เซอร์โคเนีย-อลูมิน่าและเส้นใยซิลิเคลือบด้วย ZSM-5 ที่ภาวะความดัน 2 เมกะพาสคาล อุณหภูมิ 260 องศาเซลเซียส ที่สัดส่วนของตัวเร่งปฏิกิริยาต่ออัตราการไหลของแก๊สป้อนเท่ากับ 40 กรัม.ชั่วโมงต่อโมล ซึ่งให้ค่าร้อยละการเปลี่ยนคาร์บอนมอนอกไซด์และร้อยละการเลือกเกิดแอลพีจีเท่ากับร้อยละ 59.3 และ ร้อยละ 79 ตามลำดับ

ภาควิชา	เคมีเทคนิค	ลายมือชื่อนิสิต	....
สาขาวิชา	เคมีเทคนิค	ลายมือชื่อ อ.ที่ปรึกษาหลัก	....
ปีการศึกษา	2557		

5572835423 : MAJOR CHEMICAL TECHNOLOGY

KEYWORDS: LPG SYNTHESIS / ZSM-5/SILICA FIBERS / SOL-GEL METHOD / HYBRID CATALYST / ZSM-5

WITTAWAT RATANATHAVORN: DIRECT SYNTHESIS OF LPG FROM SYNGAS OVER HYBRID CATALYST OF Cu/ZnO AND SILICA FIBER COATED WITH ZSM-5. ADVISOR: ASST. PROF. DR. PRASERT REUBROYCHAROEN, D.Eng., 90 pp.

The LPG synthesis process was performed by using hybrid catalyst of $Cu/ZnO-ZrO_2-Al_2O_3$ catalyst and ZSM-5/silica fibers. The methanol synthesis catalyst as $Cu/ZnO-ZrO_2-Al_2O_3$ was prepared by co-precipitation method and ZSM–5/silica fibers were prepared by using sol-gel method assisted with electrospinning technique followed by hydrothermal process. Tetraethyl orthosilicate and aluminium nitrate were used as Si and Al sources, respectively, for ZSM-5 synthesis by using tetrapropylammonium hydroxide as an organic base. The ZSM-5 coated on silica fibers was synthesized with different crystallization times (24, 48, 72 and 120 h), solution pH (8, 9 and 10) and Si/Al ratios (20, 40 and 60). At the appropriate conditions (crystallization time of 48 h, at 180 °C and pH 9), it achieved the ZSM-5/silica fibers with a surface area of 273 m^2/g. The ZSM-5/silica fibers offers several advantages over other forms like powder and granule catalyst such as flexibility and self-adjusting shape to fit into the channel. The catalytic activity of ZSM-5/silica fiber was tested by mixing with $Cu/ZnO-ZrO_2-Al_2O_3$ catalyst in fixed bed reactor for LPG synthesis from syngas and compared with conventional powder form catalyst. The highest CO conversion was achieved by using hybrid catalyst of $Cu/ZnO-ZrO_2-Al_2O_3$ and ZSM-5/silica fibers at the condition of 2 MPa, 260 °C with W/F=40 g.h/mol. It provided the CO conversion and LPG selectivity of 59.3% and 79%, respectively.

Department:	Chemical Technology	Student's Signature	
Field of Study:	Chemical Technology	Advisor's Signature	
Academic Year:	2014		

ACKNOWLEDGEMENTS

CONTENTS

TABLE CONTENTS

CONTENT OF FIGURES

CHAPTER I

Introduction

1.1 Statement of problem

Liquefied petroleum gas (LPG) is a mixture of hydrocarbon gases (C_3-C_4). It has environmentally benign characteristics and widely used as clean fuels. Normally, the LPG is produced from the refining process of crude oil or separated from natural gas. The alternative method for producing the LPG is directly conversion of synthesis gas. It could carry out on a hybrid catalyst containing of Cu/ZnO-ZrO_2-Al_2O_3 as a methanol synthesis catalyst and zeolites as acid catalysts. The reaction consists of methanol synthesis, methanol dehydration to dimethyl ether (DME), and DME dehydration of hydrocarbons. ZSM-5 catalyst is well known as an effective acid catalyst for the process of conversion of methanol to hydrocarbons (MTH). This is an alternative method for production of hydrocarbons that independent of crude oil. MTH converts methanol to a mixture of olefins, paraffins, and alkylaromatics, to produce the hydrocarbon mixtures in gasoline (MTG) or short chain olefins (MTO) [1-5]. The ZSM-5 zeolite (MFI structure) has the tri-dimensional pore structure of straight channels (5.6 x 5.3 Å) and intersection with zig–zag channels (5.5 x 5.1 Å), that it is capability for diffusion of lower than C9. ZSM-5 is used in several forms such as powder, particle, granule or extrudate, but these forms generate high pressure drop and poor mass transfer resulting in low product selectivity [6]. On the other hand, the fibrous catalyst had more advantages than powder and extrudate catalyst due to its low gas flow resistance with high mass transfer. ZSM-5 in a fibrous form is more preference due to its flexibility, and endless forms which is possible to adjust its shape to fit into the channel. Moreover, it also provides low resistance to flow of fluid with short diffusion distance [7].

1.2 **Objective**

1.2.1   To synthesize the Cu/ZnO catalyst and silica fiber coated with ZSM-5 as a catalyst for LPG production.

1.2.2   To study the LPG synthesis reaction of hybrid catalyst of Cu/ZnO and silica fiber coated with ZSM-5

1.3 **Scope of research**

1.3.1   Synthesis of ZSM-5 zeolite on silica fiber by using hydrothermal process.

1.3.2   Study the catalytic activity for conversion of synthesis gas to LPG by using hybrid catalyst of Cu/ZnO and silica fiber coated with ZSM-5.

1.4 **Expected outcome**

1.4.1   ZSM-5 crystals completely deposited on silica fibers as fibrous form.

1.4.2   Obtain the optimum conditions for preparing ZSM-5 coated on silica fibers.

1.4.3   Obtain the optimum conditions for operation of LPG synthesis process.

1.4.4   Obtain the hybrid catalyst of Cu/ZnO and silica fiber coated by ZSM-5 which is suitable for converting synthesis gas to LPG
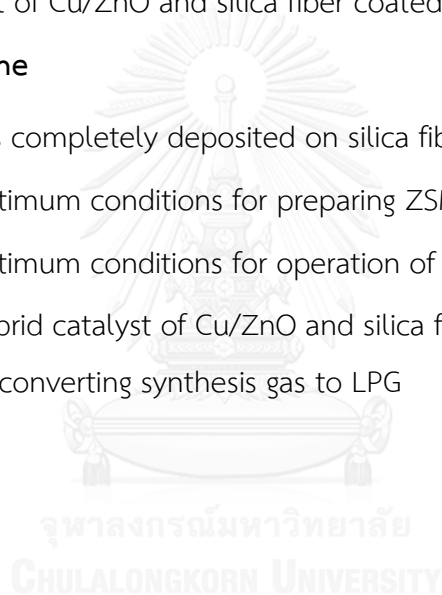
CHAPTER II

Theory and literature reviews

2.1 ZSM-5

2.1.1 ZSM-5 structure

ZSM-5, Zeolite Socony Mobil–5, is the microcrystalline aluminosilicates that consist of TO_4 which T is Si^{4+} and Al^{3+} ion and each O^{2-} is linked between T atoms and O atom lead to three-dimensional framework of TO_2 as shown in Fig. 2.1. Aluminium species in framework contains a negative charge which requires balancing cation to neutralize framework charge [8].
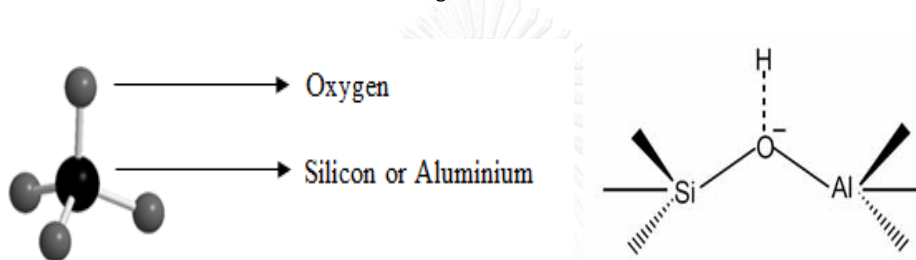
Figure 2.1 Primary structure of ZSM-5 [8]

When these primary structures are linked together by oxygen, the pentasil secondary building units ($T_{12}O_{20}$) will occur that compose of eight five-membered rings then they will form to pentasil chains. Pentasil chains are formed together via oxygen bridges resulting in complete the ZSM-5 structure which containing of 96 T-atoms and 192 O-atoms [9].

Pentasil unit   Pentasil chain   ZSM-5 structure
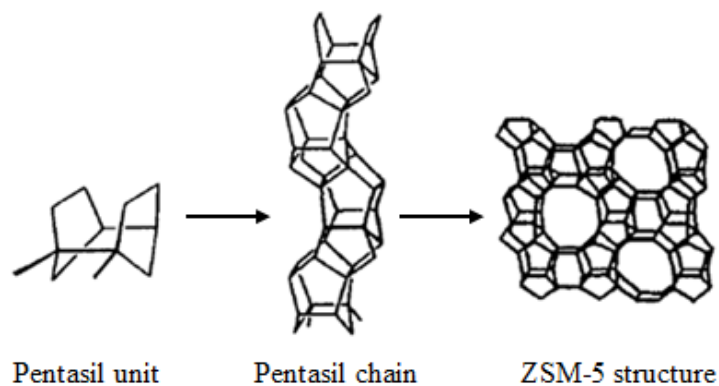
Figure 2.2 Secondary building unit and structure of ZSM-5 [9]

ZSM-5 has two perpendicular channel as shown in Fig. 2.3; the intersection straight channels are parallel to [010] plane with dimensions of 0.55 x 0.51 nm while the sinusoidal channels are parallel to plan [100] and their dimensions is equal to 0.56×0.54 nm [10]. The ZSM-5 chemical formula is $M_{x/n}$ [(AlO2)x(SiO2)y] .wH2O which "n" is the charge valence to balance cation and "w" is the number of water molecule per unit cell, and y/x is the ratio of Si/Al that are large than 5.
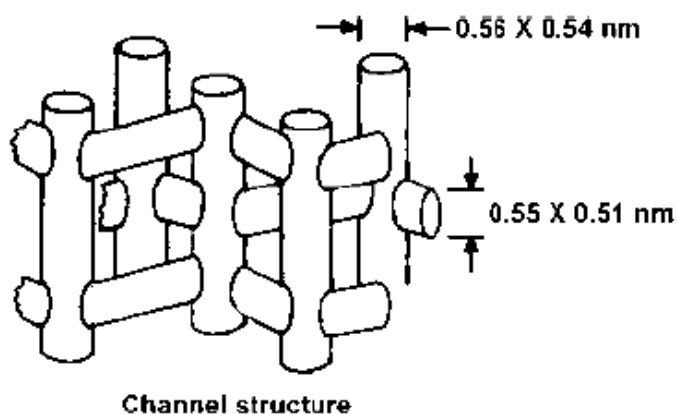
Figure 2.3 ZSM-5 porous systems [10]

2.1.2 ZSM-5 synthesis

ZSM-5 is synthesized by hydrothermal process [11, 12] the silica source, alumina source, organic template and water are mixed under high pH condition to form supersaturated sol-gel solution and are transformed to microporous crystalline aluminosilicate at high temperature. The mechanisms of zeolite synthesis were proposed by David and Lobo (1982) which are solution-mediate transport mechanism and solid phase transport mechanism. The prepared solution from the first mechanism absents of hydrogel (solid phase), the hydrated species are bounded by silicate and aluminate species then these molecules condensed and form to zeolite crystals as shown in Fig. 2.4. The second mechanism in Fig. 2.5 describes the rearrangement of solid hydrogel to form zeolite structure.

Hydrated species

OH⁻ Depolymerization

Building block

Condensation reaction

Zeolite crystals and growth of crystals

Polyhedra

Rearrangement around hydrated species
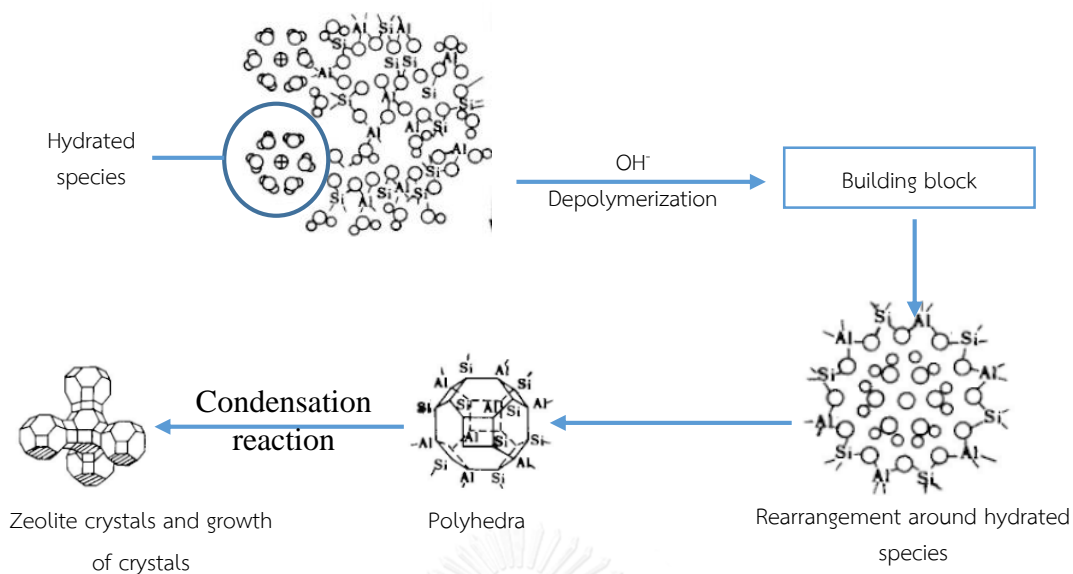
Figure 2.4 Solution-mediate transport mechanism [11]

Initial Aluminosilicate Gel

Amorphous solid phase

Liquid phase

Heating

Amorphous solid phase

Crystallizing Gel

Amorphous solid phase

1* Dissolving

Increase of concentrations in the liquid phase

Liquid phase

Condensation reactions

Growth size and number of nuclei

Accumulation of   zeolite crystals

Decrease of concentrations

Formation of nuclei

Autocatalytic growth of dissolution rate of amorphous phase

Figure 2.5 Solid phase transport mechanism [12]

2.1.2.1 The factors effect to zeolite synthesis

2.1.2.1.1 Chemical composition

Molar composition is generally offered in forms of oxide formula, SiO_2, Al_2O_3, M_xO, N_yO, R, and H_2O where M and N are alkaline metal ions and R represents organic template. These compositions have significantly effect to zeolite synthesis as shown in Table 2.1.

Table 2.1 The influences of compositions of the reaction mixture

Mole Ratio	Influence
SiO_2/ Al_2O_3	Framework composition
H_2O / SiO_2	Rate, crystallization mechanism
OH^-/ SiO_2	Silicate molecular weight
	Concentration of OH^-
Na^+/ SiO_2	Structure, cation distribution
R_4N^+/ SiO_2	Framework aluminum content

2.1.2.1.2 Aging

Aging of hydrogel could decrease the induction times by improving the nuclei formation and crystallization rate. Cundy's research [13, 14] reported that the effect of aging time to the crystallization of TS-1. The particle size tend to decrease with longer of aging period time due to increasing of nuclei. Rosilda [15] informed that the influence of the aging temperature between 25 and 180 °C on the synthesis of nanocrystal ZSM-5. They inferred that at high temperature during aging period could improve the crystal size of ZSM-5.

2.1.2.1.3 Water content for zeolite synthesis

Water content for zeolite synthesis [16] was performed as a solvent to encourage the solution mixing, materials transportation, the nucleation formation and crystal growth rate. Moreover, it showed characteristic as a stabilizer of zeolite structure by filling the pores and formed to solid solution. Generally, the dilution of the precursor mixture indicated lower supersaturated and it obtained the larger crystals.

2.1.2.1.4 Crystallization Temperature and time

Zeolite synthesis under higher temperature increases of nucleation rate, crystal growth rate and larger crystals [17]. Bhardwaj et al. synthesized zeolite by various crystallization temperature between 75 and 150°C. The amorphous phase was obtained when the crystallization temperatures are lower than 150°C. Crystallization time is a significantly parameter for zeolite synthesis. Reza et al. reported that the prepared nano ZSM-5 at different crystallization times (72, 96 and 120 h) and they concluded that longer crystallization time, crystallinity and crystal size tend to increase, due to increase in crystals nucleation and growth rate [18].

2.1.2.1.5 pH of solution

pH of solution have the effect to supersaturated silicate and aluminate species, kinetics, morphology, shape, size, and crystallinity of zeolite structure. The pH of solution is influenced by the reactants, concentrations/ratios, temperature and time. Increasing of pH will accelerate the crystal growth and a shortened of induction period before nuclei are formed.

2.1.2.1.6 Template

Template is the organic or inorganic base that use as spaces filler of zeolite structure. It encourages the formation of zeolite lattice by gelation, nucleation and decrease chemical potential (hydrogen-bonds, electrostatic and Van der waals force) of the lattice formed by the addition of the templates during zeolite synthesis.

2.1.3 Applications

Due to thermal stability, high surface area and shape selective properties of ZSM-5 thus it appropriate to use as the support or catalyst in refineries and petrochemical process that summarizes in table 2.2.

Table 2.2 Industrial applications of ZSM-5 as the catalyst

Process	Catalyst	Products
Catalytic cracking	Re-Y, US-Y, ZSM-5	Gasoline, fuels
Alkylation of aromatics	ZSM-5, Mordenite	p-xylene, ethyl-benzene, styrene
Xylene isomerization	ZSM-5	p-xylene
Catalytic dewaxing	Mordenite, ZSM-5+Ni nobel metals	Improvement of cold flow properties
Fischer–Tropsch synthesis	ZSM-5+Co,Fe, Ni	Synthesizing of hydrocarbon from synthesis gas

2.2 Silica fiber

For several years ago, many research attend to study the fibrous form of silica because its properties that can apply in many applications such as reinforcement

materials and bio sensing. Also, it can use as the support materials for packed bed reactor systems which offer a lower pressure drop and improve mass transfer of reactant in the reactor [19, 20]. The fibrous form of silica is prepared via sol-gel method followed by electrospinning technique which are described below.

2.2.1 Sol-gel process

Sol-gel [21] is the process using to prepare solid materials from solution. Sol is a colloid suspension of solid particle in a liquid and gel is a three-dimensional solid linked which pores are filled with other substances. In general, there are two main reactions which are hydrolysis reaction and condensation. The starting materials are organometallic substance in form of $M(OR)_n$ where M is metal with electron valence n, R is alkyl group with formula C_xH_{2x+1}. An example is sol-gel polymerization of tetraethoxysilane.

Hydrolysis:

$$Si(OC_2H_5)_4 + H_2O \rightarrow Si(OH)(OC_2H_5)_3 + C_2H_5OH$$

$$Si(OH)(OC_2H_5)_3 + H_2O \rightarrow Si(OH)_2(OC_2H_5)_2 + C_2H_5OH$$

$$Si(OH)_2(OC_2H_5)_2 + H_2O \rightarrow Si(OH)_3(OC_2H_5) + C_2H_5OH$$

$$Si(OH)_3(OC_2H_5) + H_2O \rightarrow Si(OH)_4 + C_2H_5OH$$

Condensation:

$$(OH)_3SiOH + OHSi(OH)_3 \rightarrow (OH)_3Si\text{-}O\text{-}Si(OH)_3 + H_2O$$

or

$$(OH)_x(OR)_ySi\text{-}O\text{-}Si(OH)_v(OR)_w \rightarrow (OH)_x(OR)_ySi\text{-}O\text{-}Si(OH)_v(OR)_w + ROH$$
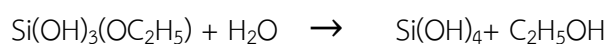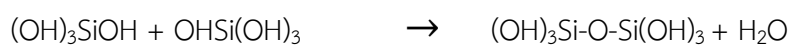
where x+y = v+w = 3

2.2.2 Electrospinning technique

Electrospinning or electrostatic spinning is a fabrication process that was first studied in 1934 [22]. This process consists of a syringe pump that assist to eject polymer solution past through the needle, metal collector and high voltage power supply as shown in Fig. 2.6. The high voltage is supplied by power supplier to generates electrical field between both electrodes, connecting the needle via wire electricity as anode and metal collector for cathode, will allow the opposite electrical charge resulting in driving of polymer jet as Taylor cone and spread onto the collector plate [23]. During the polymer ejection, the electrical charge on polymer jet was neutralized by expose with ion in the air or contact with the collector plate and the solvent was evaporated and form to solid fibers simultaneously. The fibers have a diameters ranging from several microns to lower than 100 nm. Normally, the morphology of prepared fibers and their diameters depend on the properties of polymer solution (viscosity, surface tension and conductivity), surrounding ambient parameters (temperature and humidity) and process parameters (flow rate, applied voltage, distance between tip and collector [24, 25].
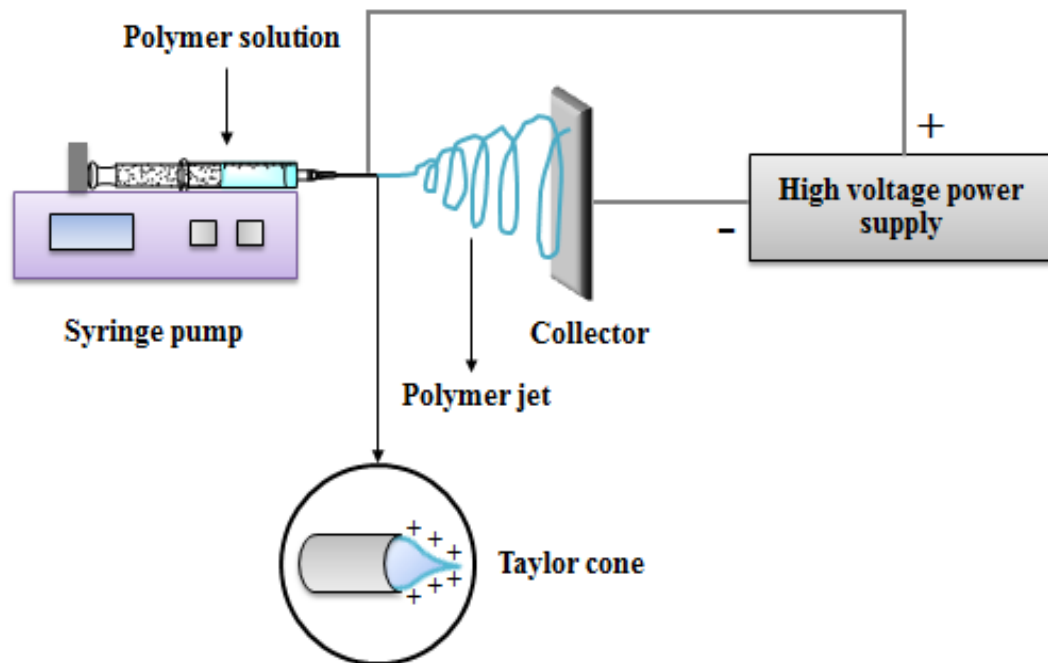
Figure 2.6 The diagram of electrospinning technique [23]

2.2.2.1 The influence of parameters for electrospinning technique

2.2.2.1.1 Viscosity/concentration

The effect of viscosity of sol-gel solution was studied by Sakai et al. At lower solution viscosity/polymer concentration, the polymer jet is abundantly with solvent causing to occur droplet and beaded formation on the collector plate. In addition, the presence of junctions and bundles has been found. The increasing of viscosity or polymer concentration provide the homogeneous fibers with lower beads and junctions, the diameter of fibers also increases. Too higher viscosity/polymer concentration, the easily drying of droplet was found and clogging at the needle tip before establishing a polymer jet. As a result, the electrospinning technique is interrupted as shown in Fig. 2.7 [26].
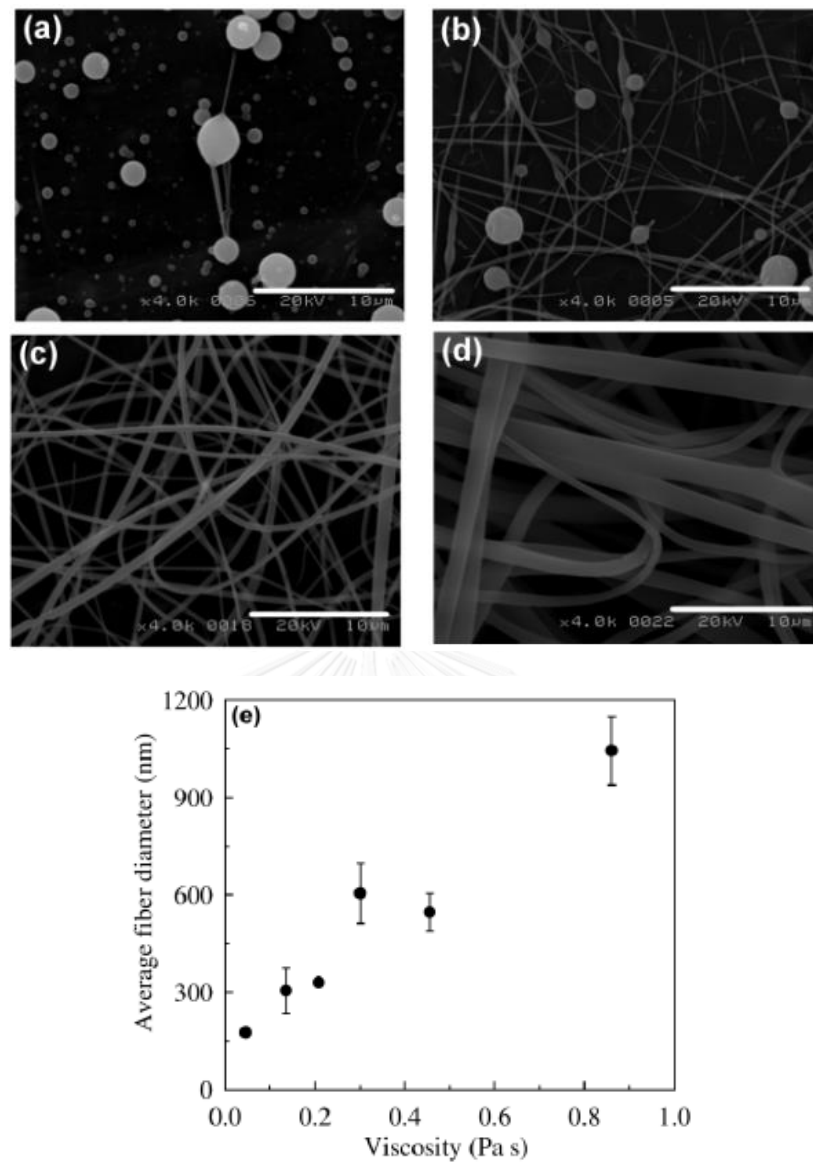
Figure 2.7 SEM image of silica fibers with various viscosities (a) 0.03, (b) 0.05, (c) 0.14, (d) 0.86 Pa.s and (e) average fiber diameters of silica fibers [26]

2.2.2.1.2 Conductivity

The conductivity properties is depends on types of solution. Using of nonionic surfactant as tetrachloromethane leads to decrease the conductivity and beads formation. Increasing of conductivity by using alcohol and volatile salt additive provide a smoother fibers surface with less beads. Small ionic surfactant can improve a mobility

and charge density so that the polymer jet has a more elongation force resulting to obtain a smaller fibers.

2.2.2.1.3 Surface tension

During the initiate step of electrospinning process, the electrical charges on polymer solution increased will be enough to outstrip the surface tension lead to stretching of polymer jet. Thus the surface tension is also significant parameter to control the spinning ability. The increasing of surface tension causing to beads formation onto the fibers. Pirzada et al. prepared a hybrid electrospun silica–PVA nanofibers with various ratios [27]. They used PVA increasing of number of entanglement in the silica solution resulting to improve the surface tension. The suitable ratio of silica to PVA indicates that the fibers with no beads and slightly size distribution.

2.2.2.1.4 Flow rate

Decreasing flow rates provides a smaller fibers because too high of flow rate lead to increase speed polymer ejection. Beads and junctions are produced because fibers still wetness during its reach to the collector plate.
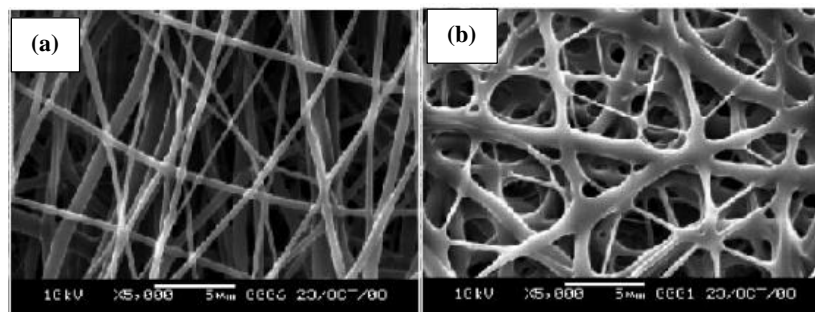
Figure 2.8 SEM images of electrospun PLGA nanofibers with different flow rates (a) 0.5 and (b) 2mL/h [27]

2.2.2.1.5 Applied voltages

Appling of high voltages causing to increase the electrical charges density on the polymer jet thus the stretching force also increase, the smaller fibers were produced. Too high voltages can decrease the Taylor cone at the tip thus the polymer jet is unstable stretched resulting to many beads on fibers are formed.

2.2.2.1.6 Tip to collector distance (TCD)

Increasing of distance between tip and collector plate can provide a smaller diameter of fibrous materials and the fibers have a more time to dry before reaching to the collector plate.

2.2.2.1.7 Ambient parameters

The temperature and humidity are the ambient parameters for electrospinning process. The increasing of ambient temperature reduce a viscosity of polymer sol causing to provide a smaller fibers diameter. The increasing of humidity effects to pores forming on fibers surface and carries about pore agglomeration [28].

2.2.3 Silica support for zeolite

Silica can be used as the support materials for various catalytic applications including with zeolite due to the presence of thermal stability, hydrophobic properties and high amount of hydroxyl group that are compatible with zeolite framework. However, silica may be loose a stability under zeolite synthesis condition so it is necessary to select the suitable condition to avoid dissolution of the support materials [29].

2.3 LPG synthesis process

Liquefied petroleum gas or liquid petroleum gas (LPG or LP gas), also referred to as mixing of propane or butane, are flammable mixtures of hydrocarbon gases used as fuel in heating appliances, cooking equipment, and vehicles. It is increasingly used as an aerosol propellant and a refrigerant, replacing chlorofluorocarbons in an effort to reduce damage to the ozone layer. When specifically used as a vehicle fuel it is often referred to as autogas. Varieties of LPG bought and sold include mixes that are primarily propane (C_3H_8), primarily butane (C_4H_{10}) and, most commonly, mixes including both propane and butane. In winter, the mixes contain more propane, while in summer, they contain more butane. Propylene, butylenes and various other hydrocarbons are usually also present in small concentrations. A powerful odorant, ethanethiol, is added so that leaks can be detected easily. The internationally recognized European Standard is EN 589. In the United States, tetrahydrothiophene (thiophane) or amyl mercaptan are also approved odorants although neither is currently being utilized.

Normally, LPG is prepared by refining petroleum or "wet" natural gas, and is almost entirely derived from fossil fuel, presence manufactured during the refining of petroleum (crude oil), or extracted from petroleum or natural gas as begin from the ground. It currently offers about 3% of all energy consumed, and burns relatively cleanly with no smoke and very few sulfur compound emissions. As it is a gas, it does not pose ground or water pollution hazards, but it can cause air pollution. LPG has a typical specific calorific value of 46.1 MJ/kg compared with 42.5 MJ/kg for fuel oil and 43.5 MJ/kg for premium grade petrol (gasoline) [30]. However, its energy density per

volume unit of 26 MJ/L is lower than either that of petrol or fuel oil, as its relative density is lower (about 0.5–0.58 kg/L, compared to 0.71–0.77 kg/L for gasoline).

Direct synthesis of LPG from syngas is an alternatively choice for converting natural gas to high-value-added products. Differently from F–T synthesis reaction mechanism [31] that the product hydrocarbons follow Anderson–Schulz–Florry distribution, the direct synthesis of LPG from syngas could be carried out over a hybrid catalyst composed of methanol synthesis catalyst and acid catalyst as zeolite [32, 33].

Cu–ZnO is lower temperature methanol synthesis catalyst, which is easily deactivated at high temperature (>300 $^\circ$C) which is the common operation temperature for syngas to LPG. Pd/SiO$_2$ methanol catalyst is expensive due to the high Pd content in the catalyst, Zn–Cr is reported to be a high-temperature methanol synthesis catalyst. The reaction of LPG synthesis consists of methanol synthesis, methanol dehydration to dimethyl ether (DME), and DME dehydration to hydrocarbons. Methanol synthesis in reaction is a rate determining step with an unfavorable of thermodynamic equilibrium. But the formations of dimethyl ether (DME) and hydrocarbons are favored by thermodynamic equilibrium. While hydrocarbons in reaction (3) could be paraffins, olefins and aromatic hydrocarbons containing of LPG in the product. The side reactions are CO$_2$ hydrogenation to MeOH and WTG reaction.

Table 2.3 The total reactions of LPG synthesis reaction from synthesis gas.

Main reactions	
MeOH synthesis	$CO + 2H_2 \leftrightarrow CH_3OH$
MeOH dehydration	$CH_3OH \leftrightarrow CH_3OCH_3 + H_2O$
DME dehydrogenation	$CH_3OCH_3 \rightarrow Hydrocarbons + H_2O$
Side reactions	
CO_2 hydrogenation	$CO_2 + 3H_3 \leftrightarrow CH_3OH + H_2O$
Water-gas Shift reaction	$H_2O + CO \leftrightarrow CO_2 + H_2$
Catalyst modifications	
Catalyst reduction	$M_xO_y + yH_2 \rightleftharpoons yH_2O + xM$

2.3.1 Cu-ZnO catalyst for methanol synthesis process

The conventional Cu/ZnO-based catalysts are prepared by a co-precipitation method developed in industry in the 1960s [34] which leads to formation of porous aggregates of Cu and ZnO nanoparticles. To form this unique microstructure, Cu-rich molar compositions of Cu:Zn near 7:3 had to be applied. Thus, the industrial system is a bulk catalyst, which is considered by a high Cu:Zn ratio with > 50 mol% Cu (metal base),approximately. The Cu nanoparticles of a size around 10 nm and ZnO particles, which are prepared in an alternating method to form a porous aggregates. These aggregates represents a large Cu surface area up to 40 m^2/g. Furthermore, industrial catalysts contain low quantities of a refractory oxide as structural promoter, in most cases up to 10% Al_2O_3. Any of the constituting elements significantly decreases the performance of the system. Significant key to obtain high performance is a large accessible of Cu surface area which has been observed to scale linearly with the

activity for samples with a similar preparation history [35]. However, between these samples considerably different intrinsic activities, activities are controlled by the Cu surface area. Thus, different "qualities" of Cu surfaces can be prepared, which vary in the activity of their active sites and/or in the concentration of these sites. Therefore, methanol synthesis over Cu catalyst appears to be a structure sensitive reaction [36]. One Significant role of ZnO is improves an effective dispersion of the Cu metallic phase [37] and increase Cu Surface areas.

However, it has been since long recognized that the role of ZnO in the final composite catalyst goes beyond that of an ordinary physical spacer between Cu nanoparticles preventing them from sintering. The presence of ZnO beneficially affects the intrinsic activity of Cu-based methanol synthesis catalysts, which is known as the Cu-ZnO synergy [38-40]. Over the past decades of Cu/ZnO research, many different models have been proposed to explainthis synergistic effect. This undissolved controversy is partially because in some cases the experimental evidence could not be obtained on the highly optimized and mature technical system, but rather on simplified model samples ranging from Cu single crystals to Cu nanoparticles supported on highly crystalline ZnO with a low loading, thus, with a composition and microstructure strongly deviating from that of the industrial catalyst described above.

2.3.2   Reaction Pathway

The reaction pathway and selectivity for hydrocarbon and oxygenate formation from the CO hydrogenation are governed by reaction conditions and catalyst compositions. A summary of these catalysts and a description of their typical selectivities. The reason for the formation of a wide range of C_1 to C_n products (i.e., C_1: methane, methanol; C_2 ethylene, ethane, ethanol, and acetaldehyde; C_3: propylene,

propane, propanol, propionaldehyde, and acetone, C_n: species containing n number of carbon atoms) can be traced to the polymerization and network characteristics of the reaction which consists of a large set of parallel and series reaction pathways, shown in Fig.2.9
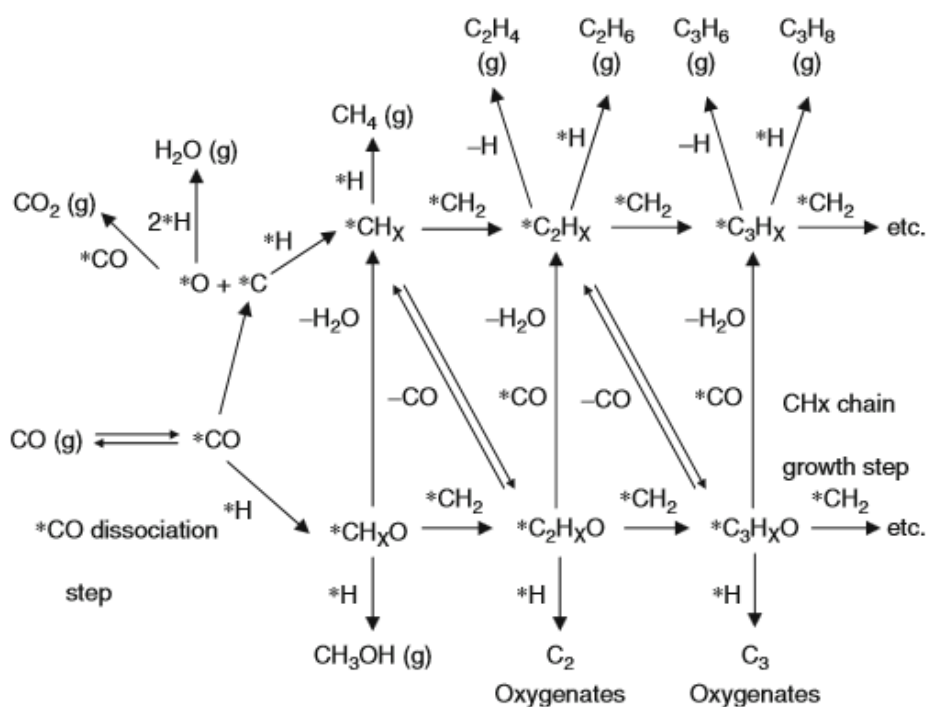
Figure 2.9 CO hydrogenation reaction mechanism [41]

The first steps in the overall CO hydrogenation reaction mechanism is adsorption of reactants, H_2 and CO. All of the CO hydrogenation catalysts have the capability to chemisorb hydrogen dissociatively, $H_2 + 2^* \leftrightarrow 2H^*$ (2*: two empty sites) and chemisorb of CO in either a non-dissociative or dissociative form. This relationship is a difference result of Fermi energy, E_f, reflecting in the ability of the metal in electron back donation to the $2\pi^*$ vacant orbital of CO as shown in Fig.2.10. This back donation would weaken the CO bond and stabilize the M–C bond. Metals such as Fe indicates E_f above the level of the $2\pi^*$ orbital, tend to dissociate adsorbed CO. In contrast,

metal such as Pd, Pt and Cu exhibit activity for chemisorbing similar to CO non-dissociation. The most direct impact of the CO dissociation activity is on the selectivity of the reaction. High CO dissociation activity favors the formation of adsorbed carbon which can further hydrogenate to form CH_x, leading to the formation of hydrocarbons such as CH_4. In contrast, poor CO dissociation activity allows adsorbed CO to be hydrogenated to methanol. Metals such as Rh in the forms of either single crystal or supported catalysts with moderate CO dissociation activity exhibited good selectivity toward C_2 oxygenates. This observation is consistent with the proposed C_2 oxygenate formation mechanism that C_2 oxygenates are produced from both dissociation and non-dissociatively adsorbed CO [41].
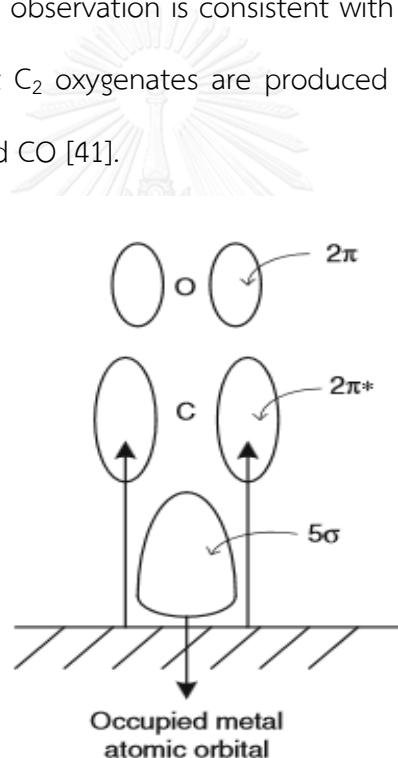
Figure 2.10 Interaction of CO with metal surfaces [41]

Water–gas shift mechanism over cobalt catalyst occurs via a reactive formate intermediate that show in Fig. 2.11. The adsorption of hydroxy species or water and carbon monoxide lead to formation of formate species and the hydroxy intermediate

can be formed by the decomposition of water. The formate species a can be reduced to carbon dioxide.
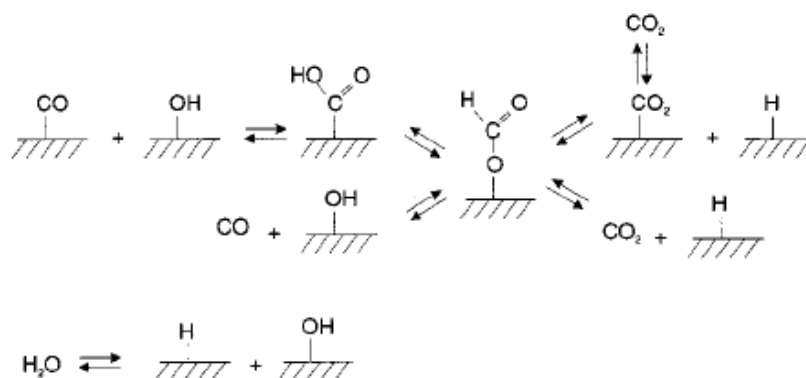
Figure 2.11 Water–gas shift reaction mechanism via formate species [35]

2.3.3 The influence of parameters

2.3.3.1 Reaction temperature

Yingjie et al. [5] studied the effect of increasing temperature on methanol conversion and fractional distribution of hydrocarbon products. At constant gaseous space time (1/GHSV) and feed partial pressure, methanol-to-hydrocarbon conversion over the H-ZSM- 5 catalyst was enhanced by increasing reaction temperature, and complete conversion of methanol occurred at temperatures higher than 435°C. The C_3-C_4 fractional formation was also favored at high temperatures with respect to the formation of C_1-C_2 hydrocarbons or total aromatics and C_{5+} non-aromatics. At low temperatures, methane content is very low. A moderate increase in reaction temperature caused thermodynamic shift of the product distribution towards the fractions of lower olefins, so butanes and especially propene became more important. In fact, the methanol to hydrocarbon reaction gradually departed from the well-known MTO reaction region. At higher temperatures, methanol conversion easily approached 100%. The C_1-C_2 fraction increased gradually and the fraction of total heavy byproducts

decreased, although large C_8-C_{10} and C_8 aromatics appeared. The difference in both light and heavy fractions is attributed to the secondary cracking of olefinic oligomers and heavy C_{5+} non-aromatics at high temperatures in the company of the acid catalyst. Methane content began to increase to a certain amount. Therefore, the optimum LPG synthesis from methanol catalyzed by the H-ZSM-5 catalyst proceeds in the range from 400 to 435°C.

2.3.3.2 Reaction Pressure

Xiangang et al. [2] studied the effect of reaction pressure on LPG synthesis. Two back pressure valves were used in two-stage reaction system to manage each stage's pressure respectively. The CO conversion and CO_2 selectivity were almost unchanged when the reaction pressure of the second stage increased from 0.5 to 2.5 MPa. It confirmed that CO conversion and CO_2 selectivity were dominated by the first stage and hardly affected by the second stage. The LPG selectivity of hydrocarbons increased first, with the increase of reaction pressure, and then fell down. Also, high pressure promoted the yield of methane. This is undesirable because methane is the most unfavorable product in this process. So the appropriate pressure of the second stage was about 1.0–2.0 MPa. In the other hand, influence of reaction pressure on LPG synthesis over Cu–Zn–Al/Pd–Y hybrid catalyst was studied in 2011. The high reaction pressure promoted CO conversion and hydrocarbons yield with a slightly change of LPG selectivity. The content of C_2 in hydrocarbons fell down with the increase of reaction pressure. However, the yield of methane increased at high reaction pressure. Furthermore, higher reaction pressure also increased the content of heavy hydrocarbons (containing more than five carbon atoms), which were destructive for

the zeolite activity. So a relatively low reaction pressure (3.0–4.0 MPa) was suitable for LPG synthesis.

2.3.3.3 SiO_2/Al_2O_3 ratio

The catalytic performance of H-ZSM-5 catalysts clearly depends on the silica to alumina ratio. The results of conversion as a function of time on-stream revealed that the deactivation of catalysts gradually increased with reduced silica to alumina ratio. Methanol conversion was relatively high compared to DME. On the other hand, the DME conversion increased gradually and then exceeded methanol conversion with increasing of silica to alumina ratio. The DME reaction behavior is different to that of methanol with greater silica to alumina ratio, and can be attributed to variations in hydrophobic property of H-ZSM-5 catalysts and the diversity in molecular polarity. The reactivity of each feed generally falls with increasing silica to alumina ratio, possibly due to reduction in the number of available active sites. Figure 4 shows the various fraction distributions related to the silica to alumina ratio. The selectivity for LPG hydrocarbons is improved with increasing silica to alumina ratio. The improvements in C_3-C_4 intermediate selectivity was associated with decreases in conversion under given reaction conditions. In addition, selectivity for both light and heavy fractions were also lower with increasing silica to alumina ratio. The monotone increase in selectivity for LPG hydrocarbons may be attributed to the decrease in acid density on the catalysts, which is a function of the silica to alumina ratio and affects the conversion depth of these oxygenates. To increase both the yield of LPG hydrocarbons and the resistance to deactivation of catalysts, H-ZSM-5 with a silica to alumina ratio of 90 was selected, in contrast with the previous work, for the following investigations. A more detailed discussion on other catalysts will be reported later.

2.3.3.4 W/F ratio

Yildiz *et al*. [42] studied the effect of the W/F (catalyst weight/feed flow rate) ratio on catalyst deactivation conditions, experiments were conducted at 3 different W/F ratios (5.5, 11.5, 17.0), and at a constant H_2/CO value of 2, temperature of 523 K, and a minimum 20% CO in feed. CO conversion was increased with increasing of the space time. Increasing of the W/F ratio caused a decrease in catalyst activity, as a function of time, due to coke formation. An increasing of methane selectivity and a decrease in C_2-C_3 hydrocarbons selectivity were observed at high W/F ratios. Furthermore, the amount of carbonaceous compounds deposited on the used catalyst increased from 17% to 35% by increasing the W/F ratio from 5.5 to 17 mg.min/mL

2.4 Literature reviews

Xiangang *et al*. [1] synthesized the LPG from synthesis gas in two-stage synthesis. Firstly, the synthesis gas is converted to DME over Cu-Zn-Al/ZSM-5 catalyst. The second stage is hydrocarbon conversion over Pd-Y catalyst. They found that the conversion of LPG would increase at the temperature below 250 °C. Hydrocarbon conversion from DME is improved at high operating temperature around 335-405 °C.

Zhang *et al.* [4] studied on the selective synthesis LPG from synthesis gas over hybrid catalysts consisting of zeolite and methanol synthesis catalyst in the fixed bed reactor. They found the Cu-Zn with USY had the high catalytic performance to synthesize LPG with LPG selective around 75%.

Q. Ge *et al*. [3] focused on the high performance hybrid catalyst for syngas to LPG, composed of Cu-ZnO methanol synthesis catalyst with low Pd content Pd-beta zeolite. The optimum condition for LPG synthesis was found at, temperature of 325-350 °C and reaction pressure of 2.1-3.6 MPa. The Cu-ZnO/Pd-b exhibited an excellent catalytic

performance for syngas to LPG with 72.2% CO conversion, 78.0% LPG selectivity in hydrocarbons, and 45.3% hydrocarbon yield.

Yang *et al.* [43] synthesized ZSM-5 with the molar ratio $1.0SiO_2$: $.25TPAOH$: $0.0125Al_2O_3$: $60H_2O$ then growth on various sizes of Co/SiO_2 pellets by hydrothermal process. The Fischer–Tropsch (FTS) reaction was employed for catalytic testing. The XRD patterns were able to confirm ZSM-5 and Co_3O_4 coating on SiO_2 surface. The smaller Co/SiO_2 pellets presented the higher ZSM-5 intensity due to large amount of ZSM-5 could be coated. BET surface area also increased with decreasing of Co/SiO_2 size. The catalyst morphology and elemental components were studied by SEM-EDS, the hexagonal crystalline of ZSM-5 was found and Co molar ratio was 9.34% that close to the original content. The catalyst acid sites were investigated by NH3-TPD. They concluded that there are similar ZSM-5 acid sites and peak intensities increased when decreased SiO_2 pellets size. Moreover it displayed higher catalytic activity of FTS reaction and provide higher selectivity of isoparaffin. Several years later,

Yang *et al.* [44] synthesized core-shell like zeolite capsule catalyst by deposition of silicalite-1 onto Co/SiO_2 then growth ZSM-5 via hydrothermal process at 180 °C 24 hours to become a final layer. The obtained catalyst was named Co/SiO_2-Z-HT. The catalytic testing was investigate by FTS reaction and compared among Co/SiO_2-Z-HT, physically adhesive method (Co/SiO_2-Z-PA) and physically mixed ZSM-5/Co/SiO_2 (Co/SiO_2-Z-M) catalyst. All the tested catalyst displayed CO conversion over 90%, the major products composed of light hydrocarbon which were n-paraffins and isoparaffin. The CH_4 selectivity was ranging from 17.5-23.7%. Co/SiO_2-Z-PA provided the highest catalytic performance whereas Co/SiO_2-Z-HT gave lowest due to the zeolite overspreading on Co/SiO_2, the reactants and products are more difficult to react with

Co. Moreover, there might be partial interaction between Co clusters with Brönsted acid site of zeolite which suppressed cracking activity during FTS reaction.

Louis *et al.* [45] synthesized ZSM-5 on glass fibrous support with 3 difference methods which are synthesizing in alkaline media without silica source, synthesizing in alkaline media without silica source and synthesizing with fluoride method. All synthesized catalysts were characterized by BET SEM and XRD and the catalyst was tested with gas-phase partial oxidation of benzene by N2O to phenol. The fluoride-containing zeolite catalysts exhibited the highest performance with benzene conversion over 20% and 98% selectivity of phenol.

Vu *et al.* [46] synthesized silicalite-1/ZSM-5 composites. ZSM-5 was synthesized under hydrothermal conditions at 180 $^\circ$C for 24 h with solution molar ratios 2.5 SiO_2 (TEOS): 1.0 SiO_2 (CS): $0.025Al_2O_3$: 0.5 TPABr: 0.25 Na_2O: 120 H_2O. The obtained product was rinsed with DI water and calcined at 600 $^\circ$C then exchanging proton with 1N of NH_4Cl for 12 h and calcined again at 600 $^\circ$C. After completely prepared ZSM-5, the silicalite-1 was prepared by mixing 0.5TPAOH: $120H_2O$: 8EtOH: $2SiO_2$ and immersed ZSM-5 into the precursor solution then using hydrothermal process at 180 $^\circ$C for 24 h to obtained the crystals. The product was rinsed with DI water for several times and dried at 90 $^\circ$C overnight then calcined in the air at 500 $^\circ$C for 5 h. The difference rotating speed is the parameter that effect to crystal sizes. Decreasing of crystal sizes resulted in increasing external surface area of ZSM-5 thus silicalite-1 are more spread on the ZSM-5 surface.

Choi *et al.* [47] prepared silica nanofibers from 1TEOS: 0.01HCl: $2H_2O$: 2EtOH. The polymer solution was stirred and heated at 80 $^\circ$C for 30 min. The distance between the tip and collector was 10 cm and the applied voltage was ranging from 10 to 16 kV. At

high applied voltage leaded to the shifting of smaller diameter distribution. The diameter was mostly ranging between 200-600 nm. From FTIR results revealed the spectrum at 795, 950, and 1058cm^{-1} belonging to Si-O vibration and showed the OH-vibration peak at 3390 cm^{-1}. This can conclude that TEOS was mostly hydrolyzed and the ethoxy group changed into the silanol group. The XRD pattern indicated the characteristic peak of amorphous silica. From TGA results showed weight loss approximate to 6.7% at 200°C owing to evaporation of solvent and at 800°C found the weight loss about 12% due to self-condensation reaction of silanol group.

Yodwanlop [48] prepared nano-electrospun silica fibers for FTS reaction by using TEOS, HCl, H2O and ethanol as the precursors then studied parameters influencing to the fibers characteristic which are diameter of needle size (0.1 and 0.25 mm.), TCD (10 - 20 cm.) and applied voltage (10-20 kV). The obtained fiber was dried in oven at 110°C for 24 h then loaded with 10-20 %wt. of Co and calcined at 400°C for 2 h. The catalytic performance was investigated under the temperature varying from 240 to 280°C. In the electrospinning step, adjusting needle size from 0.25 to 0.1 mm. lead to smaller diameter of fibers but the silica solution also clogged up at the needle easily. Moreover, the lower yield of electrospun fiber was found comparing with 0.25 mm. The appropriate TCD and applied voltage are 15 cm. and 15 kV which offered the smallest fiber with average diameter 329 nm. For FTS synthesis can conclude that the 10% wt. of Co yielded the highest FTS product selectivity and increasing in temperature to 280°C gave the highest catalytic stability and selectivity.

CHAPTER III

Methodology

3.1   **Equipment and instruments**

3.1.1 Equipment for catalyst preparation

1.   Beaker (Teflon) 100 mL

2.   Beaker (glass) 250 and 500 mL

3.   Dropper

4.   Pipette 5 and 10 mL

5.   Spatula

6.   Forceps

7.   Glass rod

8.   Cylinder 50 mL

9.   Separating funnel

10. Wash bottle

11. Crucible

12. Watch glass

13. Brush

14. Rubber pipette bulb

15. Clamp

16. Magnetic bar and Magnetic stirrer

17. Water bath

18. Syringe 3 mL

19. Needle with diameter 0.55 mm

20. Aluminum foil

21. Teflon lined stainless steel reactor

22. Wrench

3.1.2 Instruments for catalyst preparation

1. Metal collector size 20 x 20 cm

2. High voltage supplier

3. Syringe pump

4. Hydrothermal machine

5. Muffle furnace

6. Oven

7. Desiccator

3.1.3 Instruments for catalyst characterization

1. Scanning electron microscope (SEM), JEOL: JSM-6360LV

2. Energy Dispersive X-ray Fluorescence (EDX), Shimadzu: EDX-720

3. X-ray Diffractometer (XRD), Bruker: D8 Advance

4. Surface area and porosity analyzer (BET), Micromeritics: ASAP2020

5. Temperature programmed reduction (TPR)

6. Temperature programmed desorption (TPD), Autochem: 2910

7. Nuclear magnetic resonance (^{27}Al-NMR), Bruker Advance DSX500

3.1.4 Equipment and instruments for catalytic testing by LPG synthesis reaction

1. Fixed bed reactor

2. Tube furnace

3. Temperature controller

4. Thermocouple

5. Mass flow controller

6. Gas Chromatograph, Shimadzu GC-2014

7. Quartz wool

3.2 **Chemicals and Reagents**

1. Tetraethyl orthosilicate (TEOS) ≥ 99.0%, Sigma-Aldrich

2. Aluminium nitrate ($Al(NO_3)_3.9H_2O$), Univar

3. Copper nitrate nonahydrate ($Cu (NO_3)_2.9H_2O$), Sigma-Aldrich

4. Zinc nitrate hexahydrate ($ZnNO_3.6H_2O$), Sigma-Aldrich

5. Zirconyl nitrate dihydrate ($ZrO(NO_3)_2.2H_2O$), Wako

6. Palladium nitrate hydrate ($Pd(NO_3)_2.xH_2O$), Sigma-Aldrich

7. Tetrapropyl ammonium hydroxide (TPAOH) 1 M, Sigma-Aldrich

8. Ethanol (C_2H_5OH) ≥ 99.9%, CARLO ERBA

9. Hydrochloric acid (HCl) 37.0%, QRëC

10. Acetic acid (CH_3COOH), Sigma-Aldrich

11. Deionized water

12. Air zero gas 99.99%, Praxair

13. Nitrogen gas 99.99%, Praxair

14. Hydrogen gas 99.99%, Praxair

15. Gas mixture of Nitrogen 95% and Hydrogen 5%, Praxair

16. Gas mixture of Hydrogen 60%, Carbonmonoxide 32%, Carbondioxide 5% balance in Argon, BOC scientific

3.3 **Experimental Procedure**

3.3.1 Preparation of silica fibers

1) 18 ml of TEOS was mixed with 3 mL of DI water for 5 min, and then 0.01 ml of HCl was dropped into the solution and continuously stirred for 5 min.

2) Ethanol (9.72 ml) was added and stirred for 5 min following by stirred at temperature of 70 $^\circ$C for 30 min. The silica solution was stirred under the room temperature until viciousness, and then filled into the syringe and combined with the needle.

3) Installed the syringe on the pump and then connected the electrical wire to the collector plate and needle with high voltage supplier. The conditions of electrospinning were TCD 15 cm, applied voltage 20 kV, needle size 0.25 mm and spinning rate 10 mL/h. The silica solution was formed to fibers by this step.

4) The obtained silica fibers was dried in oven at 120 $^{\circ}$C overnight and calcined at 800 $^{\circ}$C for 2 h.

3.3.2   Preparation of ZSM-5 on silica fibers

1) ZSM-5 was synthesized with the Si/Al ratio of 20, 40 and 60 and solution pH of 8, 9 and 10 with molar ratio composition of 1TEOS:0.25TPAOH: xAl(NO$_3$)$_3$.9H$_2$O:80H$_2$O.

2) Silica source was prepared by adding a drop of 1M HNO$_3$ into DI water, and then added into TEOS and stirred at room temperature for 30 min followed by TPAOH and stirred at 60 $^{\circ}$C for 30 min.

3) Alumina source was prepared by mixing of Al(NO$_3$)$_3$.9H$_2$O, deionized water and TPAOH together, then stirred solution to obtain a clear solution. The alumina source was mixed with silica source and then stirred at 60 °C for 1 h. After that decreased the temperature to room temperature and stirred for 2 h and adjusted pH by acetic acid.

4) Solution with a molar ratio of 1TEOS:0.25TPAOH:80H$_2$O was prepared as the procedure in 3.3.2.1 and dropped onto silica fibers and dried the fibers at 60 °C for a few minutes.

5) Silica fibers were loaded into autoclave reactor with prepared solution. Hydrothermal process was performed under the conditions of 180°C for 24, 48, 72 and 120 h with static condition. As-synthesized catalyst was rinsed by deionized water and dried overnight and then calcined at 550 °C for 2 h.

6) The 0.1wt% of Pd was loaded onto ZSM-5/silica fibers to promote the H$_2$ spillover on catalyst surface by impregnation method and then calcination at 450 °C for 2 h to remove impurity.

3.3.3   Preparation of Cu/ZnO-ZrO$_2$-Al$_2$O$_3$ (CZZA) catalyst mixed with Pd-ZSM-5/silica fibers

1) The CZZA catalyst was prepared by co-precipitation method with the mass composition of 6:3:0.5:0.5 by dissolving the nitrate compound of copper, zinc, zirconium and aluminum in deionized water.

2) The metal precursors were simultaneously dropped with a controlled feeding rate of around 10 mL/min at 65 °C. The pH of the solution was controlled at around 6.7-7.1.

3) The synthesized methanol synthesis catalyst was further aged for 10 hour and then washed by deionized water. The synthesized catalyst was calcined at 450 °C for 2 h.

4) The synthesized CZZA catalyst was sieved to particle size in the range of 1.2 to 1.7 mm before mixed with synthesized Pd-ZSM-5/silica fiber in the ratio of 1:1.

3.3.4   Characterization

1. Scanning electron microscope (SEM)

Morphology, crystal size and coating of ZSM-5 on silica fibers were studied using JOEL model JSM-6480LV Scanning electron microscope.

2. N$_2$-sorption measurements (BET)

Surface area and pore volume of synthesized ZSM-5/silica fibers were measured by N$_2$-adsorption (Micromeritics, model: ASAP 2020)

3. X-ray Diffractometer (XRD)

XRD pattern of synthesized ZSM-5/silica fibers and Cu/ZnO-ZrO$_2$-Al$_2$O$_3$ catalyst were observed by Bruker AXS model D8 Advance, equipped with a CuKα. The scanned angle (2θ) was starting from 5 to 50 degree for ZSM-5/silica fibers and 5 to 80 degree for Cu/ZnO-ZrO$_2$-Al$_2$O$_3$ catalyst. The Co crystal size was calculated from Scherrer equation that showed below.

$$\text{Average crystal size} \ = \ \frac{K\lambda}{\beta \cos\theta_B}$$

Where

K   =   Scherrer constant

λ =   Wavelength of x-ray (Cu, Kα = 0.15406 $\overset{\circ}{A}$)

β =   Line broadening at half the maximum intensity (FWHM)

θ_B =   Bragg angle

4. Energy Dispersive X-ray Fluorescence (EDX)

Elemental components of synthesized ZSM-5/silica fibers and CZZA catalyst were detected by Energy Dispersive X-ray Fluorescence (Shimadzu, model: EDX-720)

5. Nuclear magnetic resonance (NMR)

^{27}Al-MAS-NMR measurements were performed on Bruker Advance DSX500 spectrometer with a ^{27}Al frequency of 130.4 MHz. Single pulse excitation was performed with a recycle delay of 1 s and a pulse length of 1 ms. The spectra window was 250 kHz and the spinning speed 13 kHz. The ^{27}Al chemical shifts were referenced externally to a 1 M aqueous solution of Al(NO$_3$)$_3$.9H$_2$O.

6. Temperature programmed desorption of ammonia (TPD)

The acidity was measured by ammonia adsorption–desorption technique using a chemical adsorption instrument of Autochem 2910 instrument (Micromeritics). The samples were outgassed at 500 °C in a helium flow for 1 h, then cooled to 150 °C and adsorbed NH$_3$ until saturation, the desorption began from 150 to 600 °C with constant rate of 10 °C min^{-1}.

7. Temperature programmed reduction of hydrogen (TPR)

Reduction temperature and reducibility of CZZA catalyst was carried out by using 0.1 g of catalyst was heated up to 100 °C with heating rate 10°C/min and flowed N$_2$ with flow rate 30 mL/min for 30 minutes to remove moisture and impurity. After this period, the N$_2$ flux was replaced by 5% of H$_2$ balanced with N$_2$. The temperature was heated from 100 to 400 °C with heating rate 3°C/min to reduce the catalyst. The percent of reduction of CZZA catalyst can be calculated as follow equation.

$$\% \text{ reduction } = \frac{\text{H}_2 \text{ consumption }_{\text{measured}}(\text{mol})}{\text{H}_2 \text{ consumption }_{\text{calculated}}(\text{mol})} \times 100$$

3.4 LPG synthesis process

1. 1 g of mixed CZZA and Pd-ZSM-5/silica fibers catalyst was packed into fix bed reactor.

2. Mixed CZZA and Pd-ZSM-5/silica fibers catalyst was reduced under H_2 gas (100 mL/min) at atmospheric pressure, 250 °C for 2 hours.

3. Set the temperature of furnace to desired reaction temperature (260, 270 and 280 °C). After that, synthesis gas (H_2/CO with ratio 2:1) was fed with desired W/F ratio (10, 20 and 40 g.h/mol) at the reaction pressure of 1, 2 and 3 MPa.

4. The gaseous products were analyzed continually for 5 hours by GC equipped with thermal conductivity detector (TCD) equipped with a Unibead C column to analyze gaseous with CO, CH_4, and CO_2 and flame ionization detector (FID) equipped with a capillary column for analyzing hydrocarbon gaseous produce which had GC conditions as showed in table 3.1

Table 3.1 The conditions for GC analysis

Carrier gas	99.999 % of N_2
Column type	TCD: Unibead C FID: Capillary column
Injection temperature	60 °C
Column temperature	Temperature program 130 °C, 7.0 minutes 200 °C, 17.0 minutes (rate 15 °C /min)
Detector type	TCD, FID
Detector temperature	200 °C
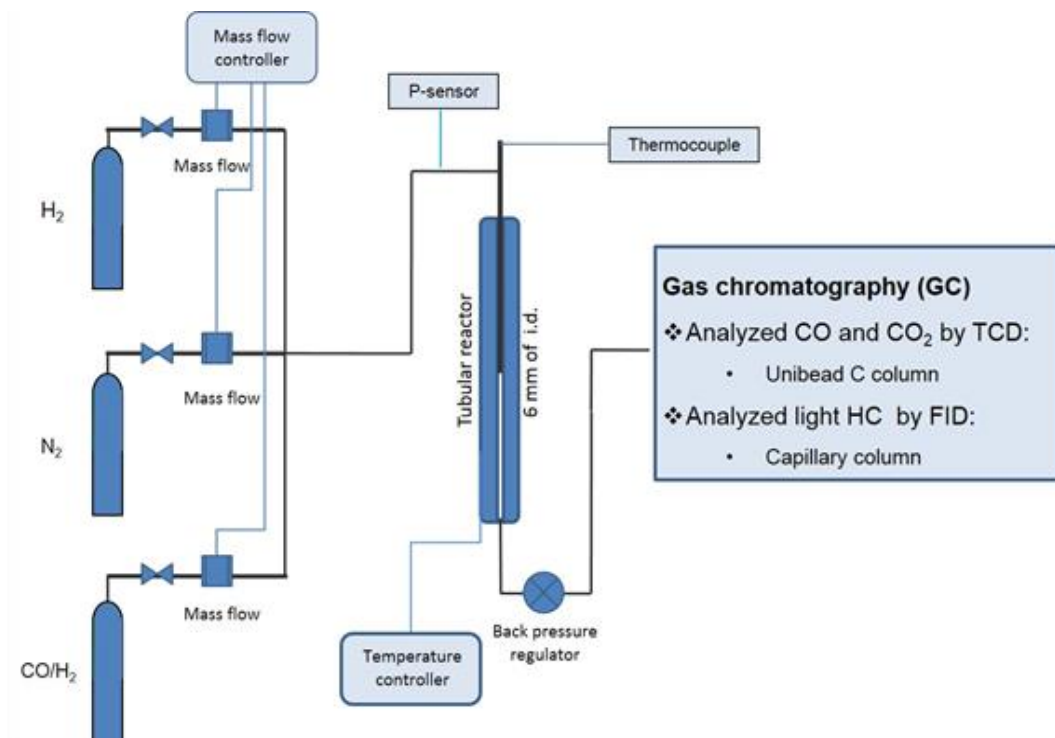
Figure 3.1 Equipment and instrument diagram for LPG synthesis process

3.5   Catalytic testing parameters for LPG synthesis process

1. Operating conditions: temperature, pressure and W/F ratio

2. Si/Al ratio: 20, 40 and 60

CHAPTER IV

Results and discussion

4.1 The study of silica fibers core materials

4.1.1   The prepared of silica fibers

The surface morphology and the diameter of prepared silica fibers prepared by using electrospinning technique with needle size of 0.25 mm, TCD of 15 cm, applied voltage 20 kV and ejection rate of 10 mL/h were observed and measured by SEM. The obtained silica fibers are rather smooth with an average diameter of 0.68 µm measuring by SemAfore program. The size distribution of diameters is ranging from 0.49 to 0.95 µm that illustrated in Figure 4.1.
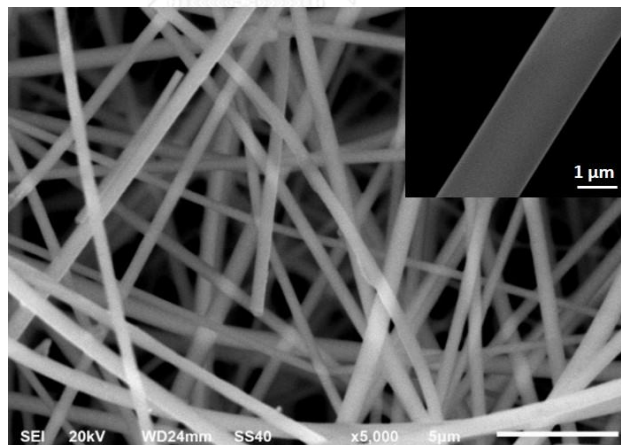
Figure 4.1 SEM image of silica fibers prepared under electrospinning condition by using 0.25 mm of needle with TCD 15 cm, applied voltage 20 kV and spinning rate 10 mL/h.

The XRD pattern was used to characterize crystal structure of prepared silica fiber as shown in Figure 4.2. As the result, the prepared silica fibers demonstrated the amorphous structure of silica pattern [51]. From BET surface area, it indicated that

prepared silica fibers considerably a low surface area approximately of 3.80 m²/g and pore volume of 0.002 cm³/g due to the nature of their non-porous structure which provides only external surface area.
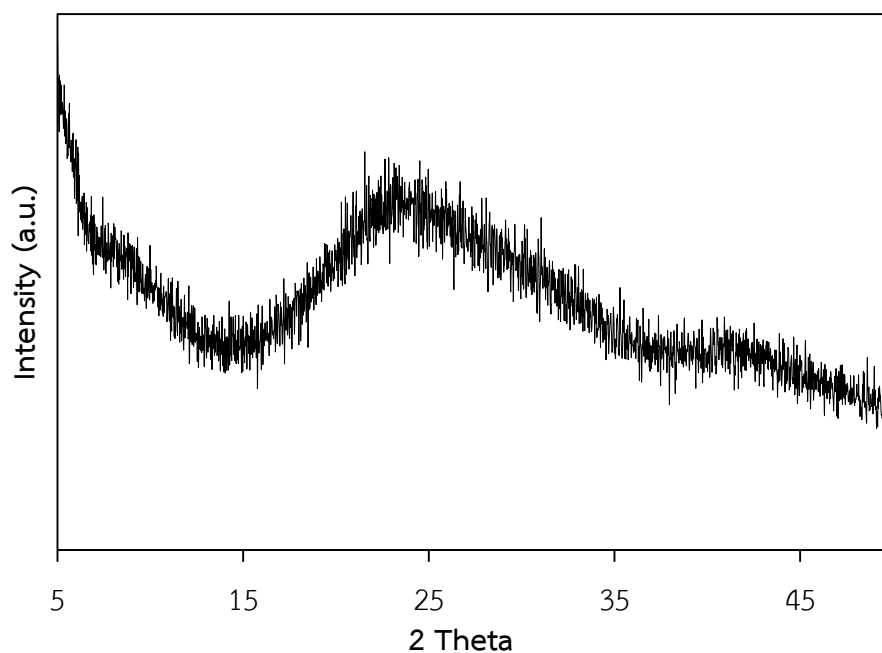
Figure 4.2 XRD pattern of amorphous silica fibers

4.1.2 The properties of commercial ZSM-5

The characteristic and properties of commercial ZSM-5 in the form of ammonium was studied the by using HSZ-800 (840NHA). It is aluminosilicate zeolite with the Si to Al ratio of 20 changing to proton form (H-ZSM-5) by calcination at 550 $^{\circ}$C for 5 h. The crystal morphology was observed by SEM as shown in Figure 4.3. From the results, it showed the hexagonal crystal shape. It had averaged crystal size of about 3.58 μm. The crystal structure of commercial ZSM-5 was confirmed by XRD pattern as shown in Figure 4.4. XRD pattern of ZSM-5 compose of two characteristic peaks at 2θ

between 7-10 and 22-25 corresponding to be the MFI structure. The physical properties including surface area, total pore volume, pore diameters and average particle size are summarized in table 4.1.

Table 4.1 The properties of commercial ZSM-5 as HSZ-800 (840NHA)

Properties	HSZ-800 (840NHA)
Si/Al	20
Surface area (BET, m^2/g)	433.8
Total pore volume (cm^3/g)	0.225
Pore diameter (Å)	20.690
Crystal size (µm)	3.58
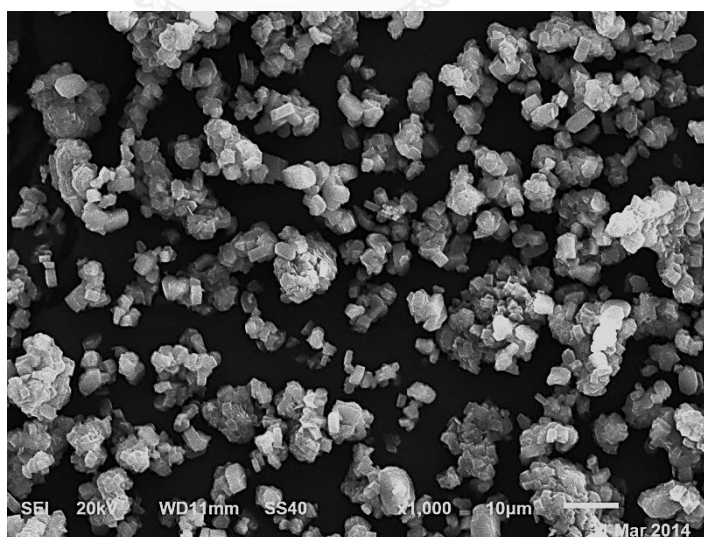
Figure 4.3 SEM image of commercial ZSM-5 with Si/Al 20
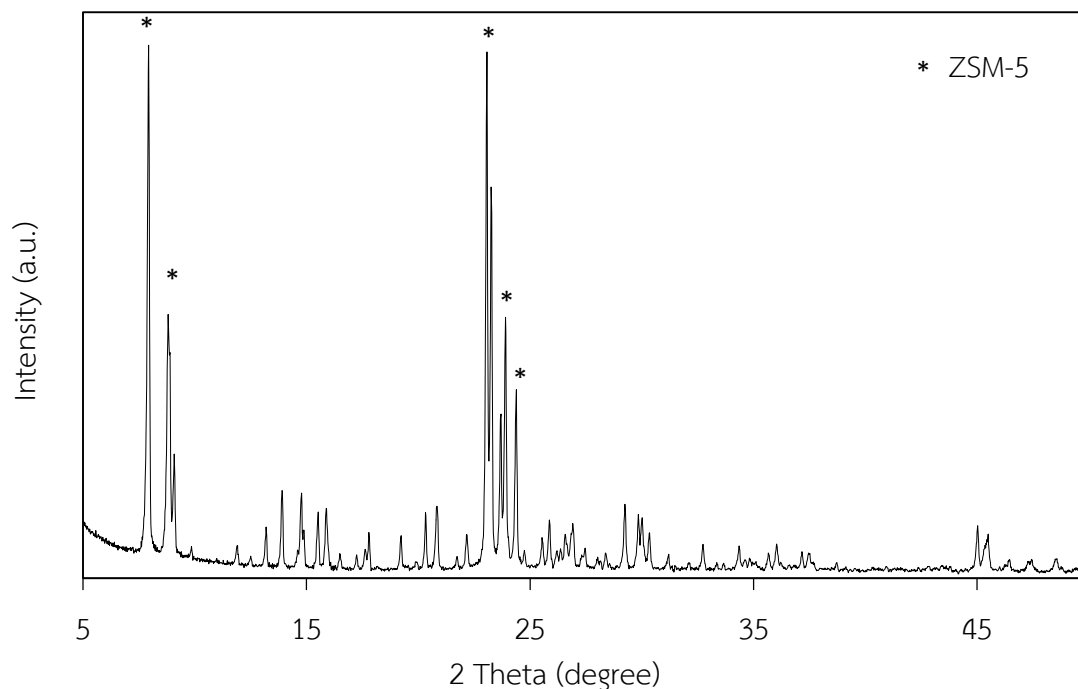
Figure 4.4 XRD pattern of ZSM-5 commercial

4.2 **The preparation of ZSM-5/silica fibers**

4.2.1   The effect of pH

The influence of pH solutions for ZSM-5 synthesis on silica fibers was studied by various pH of solution at 8, 9 and 10 with the Si/Al ratio of 40 under hydrothermal conditions at 180 °C for 24 h. Increasing of pH leads to supersaturated of silicate and aluminate species that improve a more nucleation rate and crystallization causing to reduce a crystal size of ZSM-5 on the silica fibers as shown in Figure 4.5. The XRD patterns of synthesized ZSM-5 on silica fibers with different pH at 8, 9 and 10 were shown in Figure 4.6. It indicated that all synthesized sample exhibited the MFI pattern and relative intensity tend to increase with increase the pH according to increasing of crystal size from 1.63 to 2.32 μm. BET surface area of synthesized ZSM-5 on silica fibers

increased with increase pH of solution from 70.58 to 194.30 m^2/g due to a smaller of

crystal size whereas pore size tends to decrease that show in table 4.2. Although

synthesizing under high pH obtained a more yield of ZSM-5 coating on silica fibers but

the dissolution of silica fibers during hydrothermal process also dramatically increase

especially at pH 10 [49] thus ZSM-5/silica fibers preparation at pH 9 is the suitable

condition for synthesis of ZSM-5 on silica fibers.
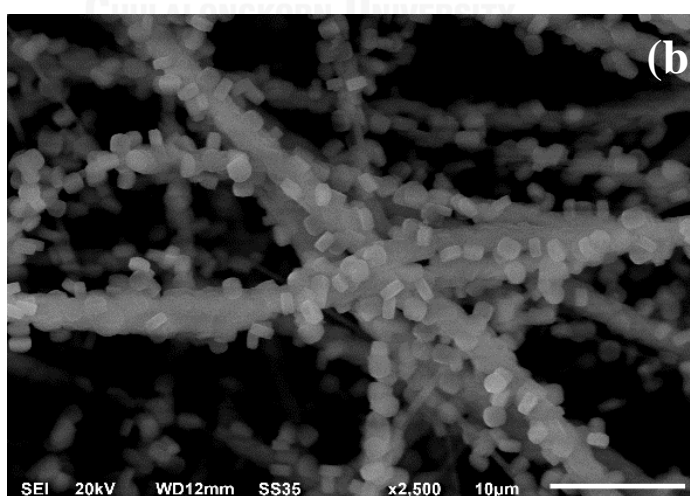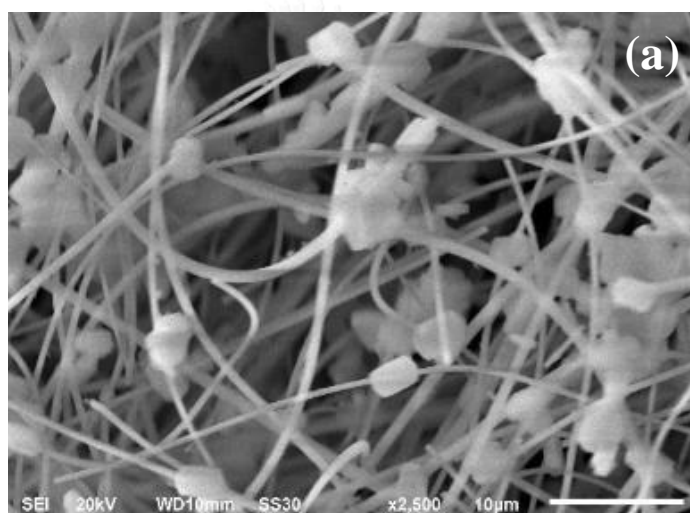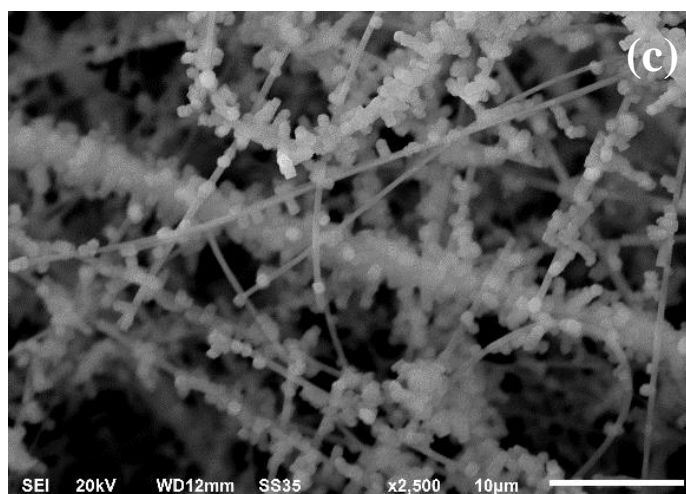
Figure 4.5 SEM images of ZSM-5/silica fibers with different pH of (a) 8, (b) 9, and (c) 10 with the Si/Al ratio of 40 under hydrothermal conditions at 180 $^{\circ}$C for 24 h.

Table 4.2 Crystal size, BET surface area, pore size and pore volume of synthesized ZSM-5/silica fibers with different pH of 8, 9 and 10.

pH	Crystal size (SEM, μm)	Surface area (BET, m^2/g)	Averaged pore size (Å)	Averaged pore volume (cm³/g)
8	2.32	70.58	43.46	0.077
9	1.74	189.04	24.81	0.117
10	1.63	194.30	26.09	0.127
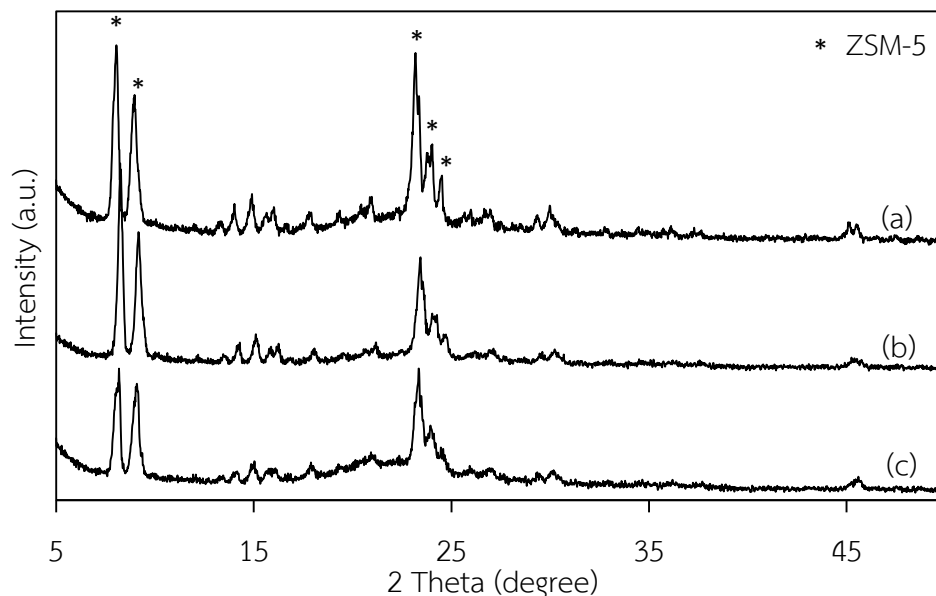
Figure 4.6 XRD patterns of ZSM-5/silica fibers with different pH of (a) 8, (b) 9, and (c) 10 with the Si/Al ratio of 40 under hydrothermal conditions at 180 °C for 24 h.

4.2.2 The effect of Si/Al ratio

The influence of Si/Al ratio for ZSM-5/silica fibers was investigated with different Si/Al ratios of 20, 40 and 60 under hydrothermal condition of pH 9, 180 °C for 24 h. In Figure 4.7 (a) to (d), it shows the SEM images of ZSM-5/silica fibers morphology with different Si/Al ratios. The crystal sizes of ZSM-5/silica fibers had a slightly difference ranging from 1.74 to 1.78 μm according to the intensity signals of XRD pattern as shown in Figure 4.9. At the Si/Al ratio of 20, it provided the lowest surface area is 70.74 m^2/g observing the lowest crystal amount on silica fibers. Because at the low ratio, a more Al species reduce the nucleation rate causing to yields of ZSM-5 crystal on silica fiber decreased.
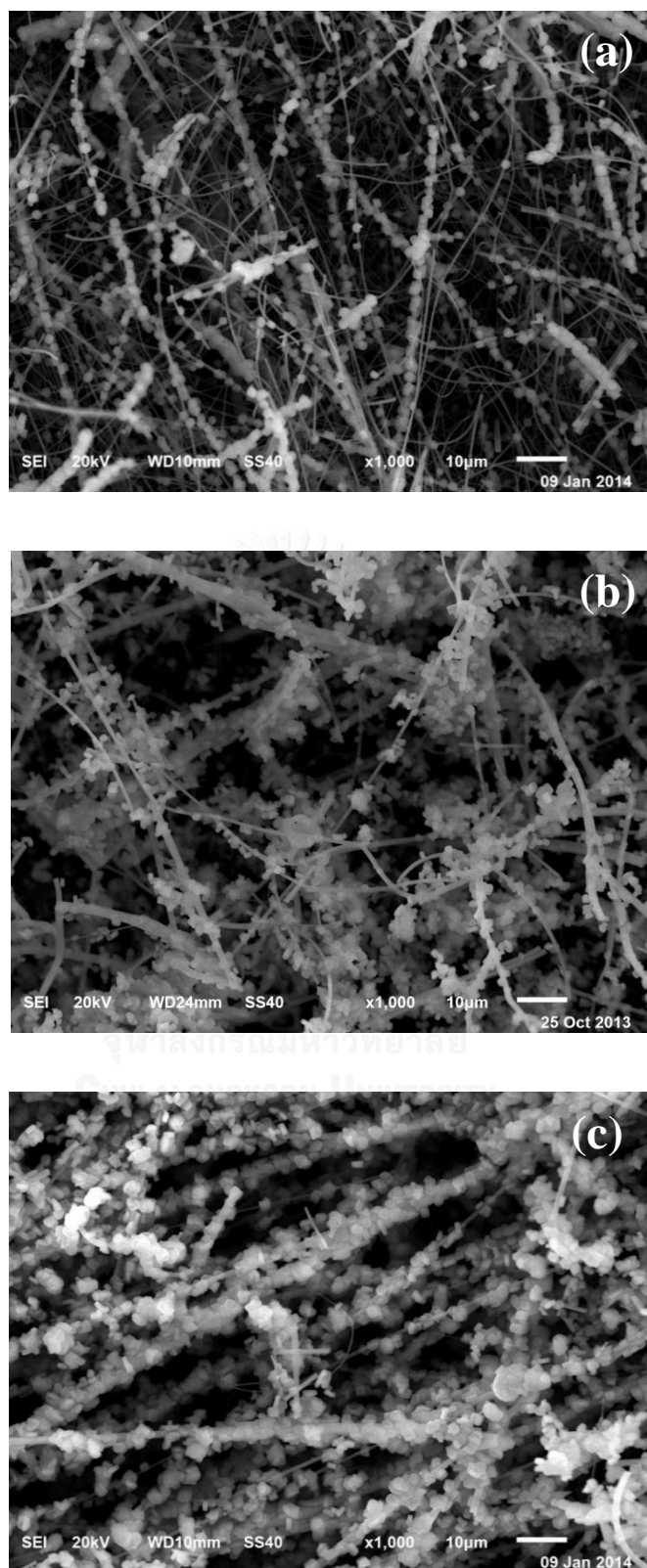
Figure 4.7 SEM images of ZSM-5 on silica fibers with different Si/Al ratios of (a) 20, (b) 40, and (c) 60 under hydrothermal condition of pH 9, 180 $^\circ$C for 24 h

Also the ratio of 40 and 60, it provided the higher surface area. The pore volume had the similar trend with surface area ranging from 0.051 to 0.157 cm^3/g, the decreasing of Si/Al ratio resulting to lower pore volume as shown in table 4.3.

Table 4.3 Crystal size, BET surface area, pore size and pore volume of ZSM-5/silica fibers with different Si/Al ratios under hydrothermal condition of pH 9, 180 $\degree$C for 24 h.

Si/Al	Crystal size (SEM, μm)	Surface area (BET, m^2/g)	Averaged pore size (Å)	Averaged pore volume (cm^3/g)	Acid amount (mmol/g)		
					Weak acid	Strong acid	Total acid
20	1.76	70.74	29.09	0.051	0.043	0.121	0.164
40	1.74	189.04	24.80	0.117	0.023	0.123	0.146
60	1.78	188.50	33.49	0.157	0.016	0.130	0.146

From the NH_3-TPD result in Figure 4.8, it shows the acidity of ZSM-5/silica fibers with different Si/Al ratios. There are only two peaks found in measurement. The first peak occurred in low temperature region between 180 and 320 $\degree$C indicating to weak acidity of the Brønsted acid sites. The acid site was formed by Al-Si atoms by bridging of hydroxyl group where the produced negative charge is compensated by proton. The second peak was found in the high temperature region over 500 $\degree$C and indicated to

hydroxyl group on surface of silica fibers. At the Si/Al ratio of 20, it provided the highest total acid amount of 0.164 mmol/g. So the acidity of ZSM-5/silica fibers related to aluminum content and increased with increasing of aluminum content in the zeolite as shown in table 4.3.
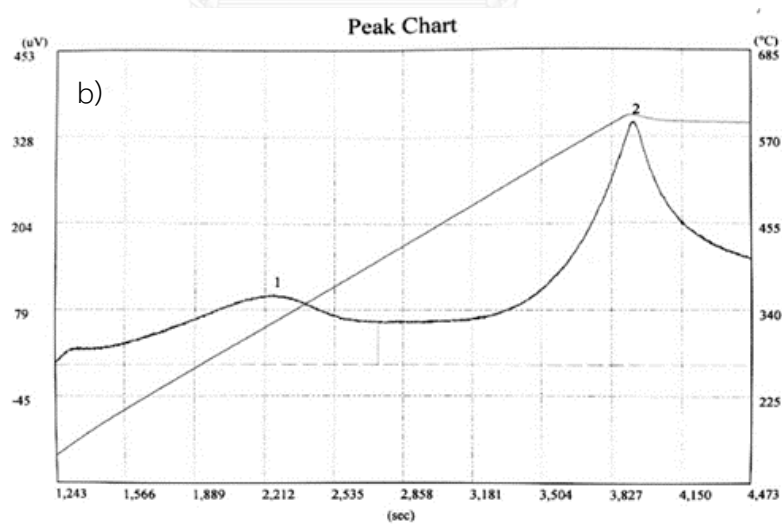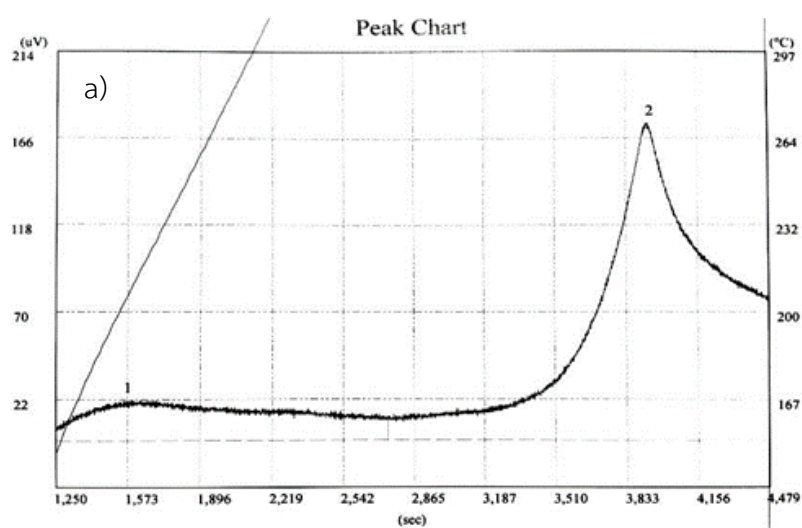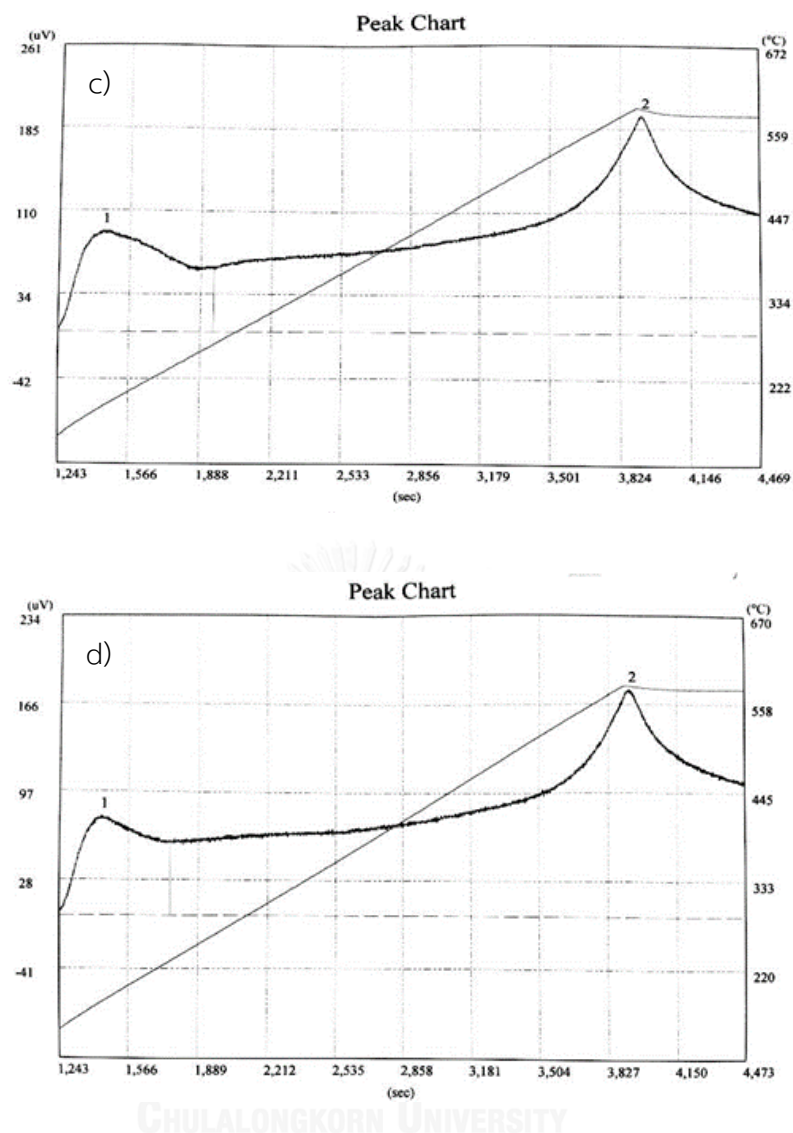
Figure 4. 8 NH$_3$-TPD profile of ZSM-5/silica fibers with different Si/Al ratios of (a) silica fibers, (b) 20, (c) 40, and (d) 60 under hydrothermal condition of pH 9, 180 $^\circ$C for 24 h
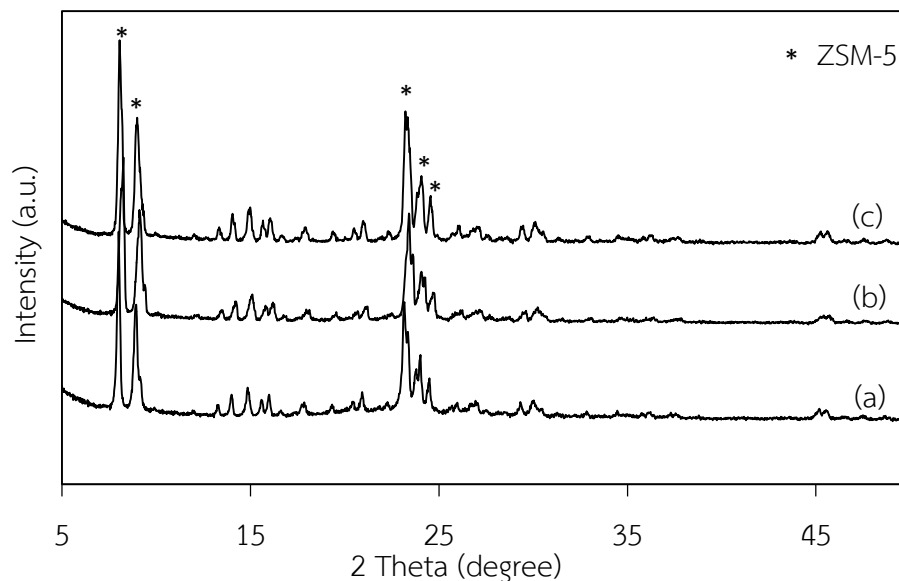
Figure 4.9 XRD patterns of ZSM-5/silica fibers with different Si/Al ratios of (a) 20, (b) 40, and (c) 60 under hydrothermal condition of pH 9, 180 $^{\circ}$C for 24 h

4.2.3   The effect of crystallization time

The influence of crystallization times for synthesis of ZSM-5/silica fibers was investigated at 24, 48, 72 and 120 h under hydrothermal condition of pH 9, 180 $^{\circ}$C. The SEM image in Figure 4.10(a) to (d) presented the ZSM-5 coating on silica fibers with increase the crystallization time. The crystal sizes were increased with increased the crystallization times from 1.74 to 3.22 μm according to relative intensity of XRD pattern in Figure 4.11. From this result, it also provided the increasing of surface area and pore volume while the pore size had a slightly difference. Because the increasing of crystallization time causing to improve the nucleation and crystal growth. The nucleation rate was significantly increased during the first 48 h, resulting to generate a more nuclei causing to increase a nuclei formation on silica fibers observing from SEM

image in Figure 4.10(a-b). While the crystal growth rate significantly increased after 48 h to 120 h causing to increase a larger crystal size.

During the first 24 h of crystallization time, it was observed that ZSM-5 crystal growth incompletely enclosed on silica fibers due to less nucleation rate as shown in Figures 4.10(a). At 48 h of crystallization time, it was indicated the deposition of ZSM-5 covered all silica fibers surface, which the structure was similar to Tinospora crispa as shown in Figures 4.10(b). BET surface area of 48 h of crystallization time provided surface area of 273 m^2/g. Although, crystallization time at 120 h, ZSM-5 crystal over grew on silica fibers which loosed their fibrous characteristic as shown in Figures 4.9(d). Thus, crystallization time of 48 h was the most suitable for ZSM-5 deposited on silica fibers. Figures 4.10(b) shows the surface morphology of Tinospora crispa-like ZSM-5/silica fibers. ZSM-5 crystal presented single hexagonal crystalline nanoparticle with the size of 1.8 μm distributed along silica fibers. Since the surface of silica fibers composed of SiO_2 as a silica source, it could form Si-O-Al cross-link between silica fibers and ZSM-5 led to the ZSM-5 crystallite, completely deposited around fiber surface.
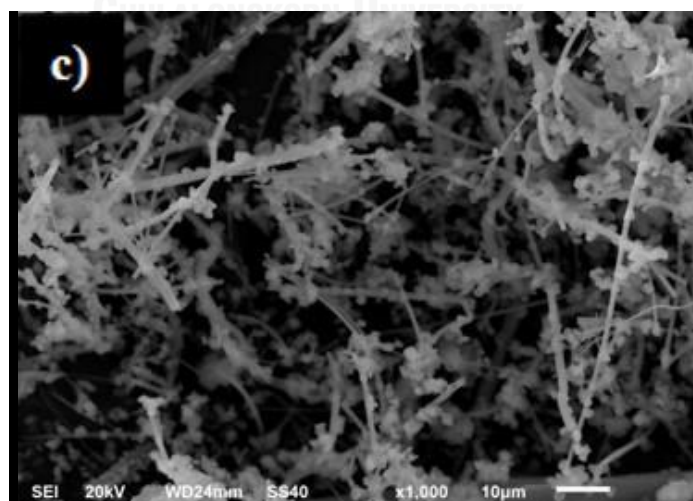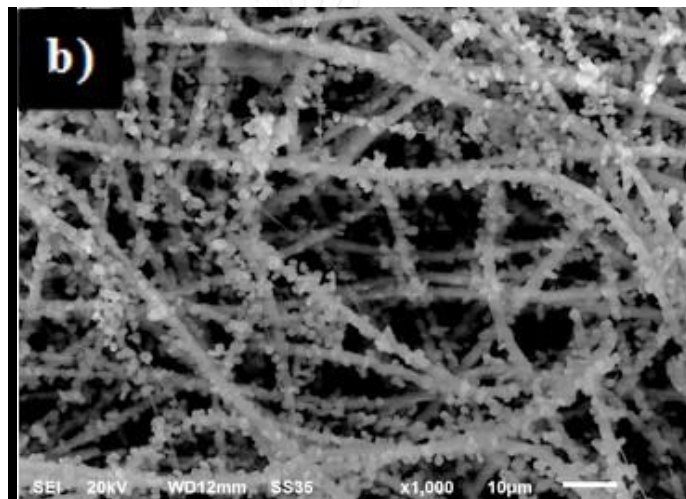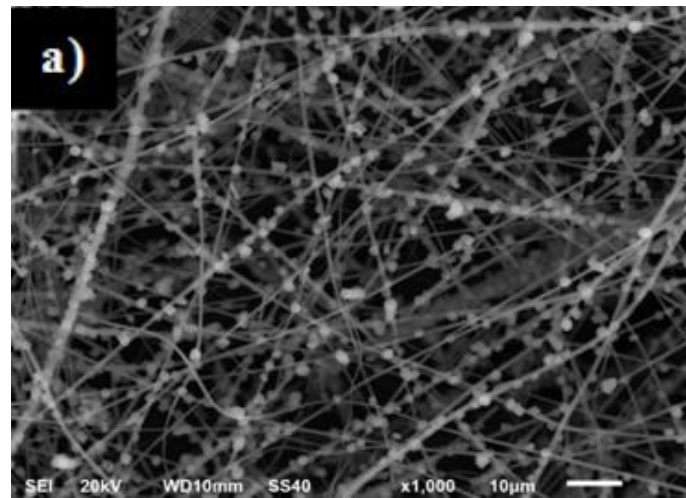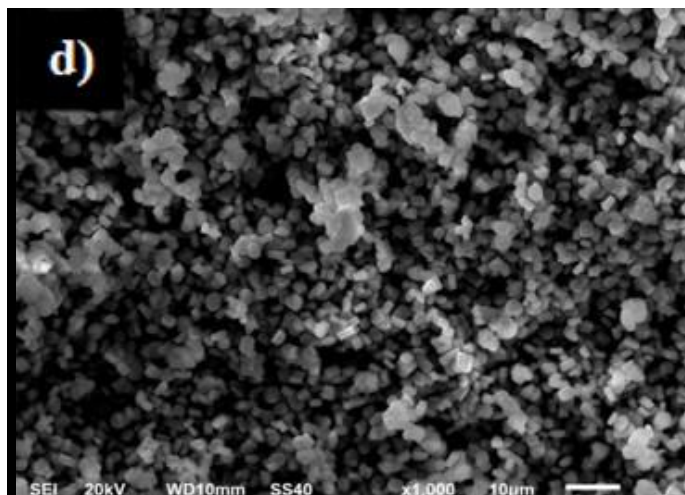
Figure 4.10 SEM images of ZSM-5/silica fibers with different crystallization times of (a) 24 h, (b) 48 h, (c) 72 h, and (d) 120 h under hydrothermal condition of pH 9, 180 °C

Table 4.4 Crystal size, BET surface area, pore size and pore volume of ZSM-5 on silica fibers with different the crystallization times under hydrothermal condition of pH 9, 180 °C

Time (h)	Crystal size (SEM, μm)	Surface area (BET, m^2/g)	Averaged pore size (Å)	Averaged pore volume (cm^3/g)
24	1.74	189.04	24.806	0.117
48	2.58	273.00	25.273	0.172
72	2.67	326.45	25.048	0.204
120	3.22	436.80	20.69	0.225
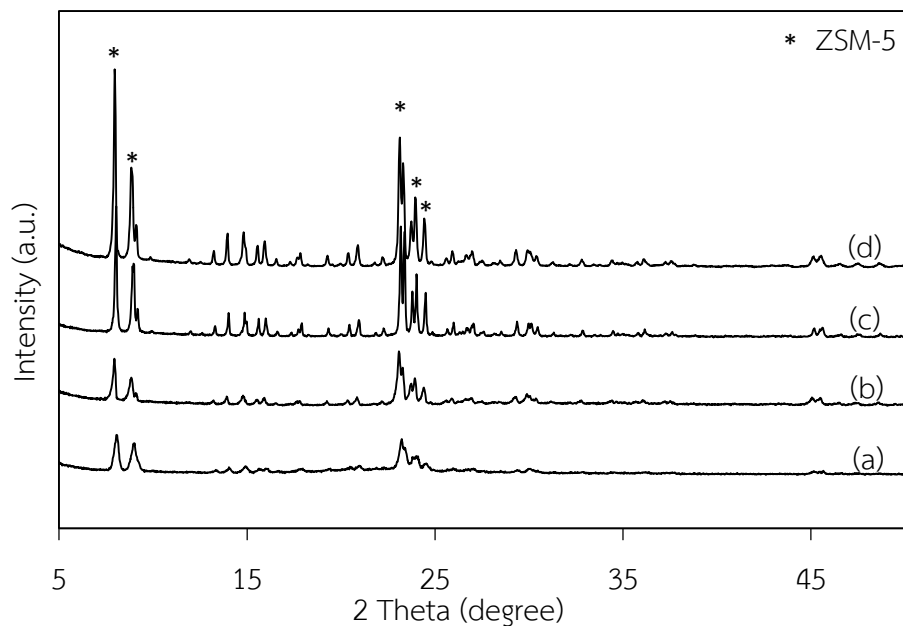
Figure 4.11 XRD patterns of ZSM-5 on silica fibers with different crystallization times of (a) 24 h, (b) 48 h, (c) 72 h, and (d) 120 h under hydrothermal condition of pH 9, 180 °C

In Figure 4.12, it showed the nitrogen adsorption isotherm of synthesized ZSM-5/silica fibers with different crystallization times. The isotherm of silica fibers (Figure 4.12a) indicated the type II isotherm with low gas adsorption volume and absence of hysteresis indicates adsorption on and desorption from a non-porous surface confirming that silica fibers was a non-porous structure with low surface area. All of commercial ZSM-5 and synthesized ZSM-5/silica fibers with different crystallization times exhibited the steep initial region due to very strong adsorption with microspores indicating to be the isotherm type I or pseudo-Langmuir.
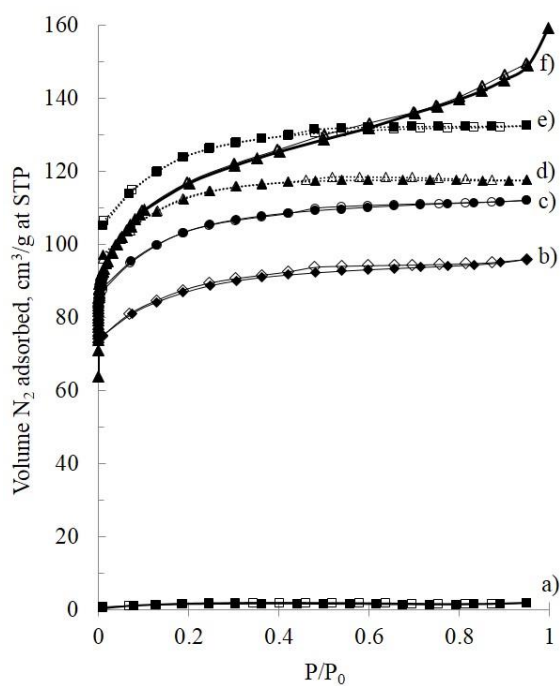
Figure 4.12 Nitrogen adsorption isotherm of (a) silica fibers, ZSM-5/silica fibers synthesized for (b) 24 h, (c) 48 h, (d) 72 h, and (e) 120 h, and (f) commercial ZSM-5.
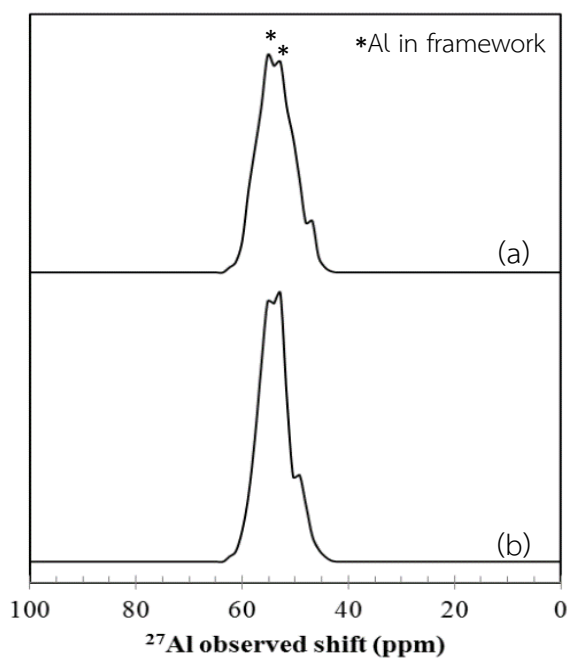
Figure 4.13 ^{27}Al MAS NMR single pulse spectra of (a) ZSM-5/silica fibers synthesized at pH 9, 180 $^{\circ}$C for 48 h comparing with (b) commercial ZSM-5 with Si/Al=20.

The gas adsorption volume of ZSM-5/silica fibers was improved with increasing of crystallization times from 24 to 120 h which demonstrates the microporous structure of ZSM-5/silica fibers obtained from the typical pore structure of ZSM-5 deposited on silica fibers. The gas adsorption volume of ZSM-5/silica fibers was nearly one hundred times that of the pure silica fibers.

In Figure 4.13, it showed the ^{27}Al NMR spectra of ZSM-5/silica fibers synthesized under the hydrothermal conditions of pH 9, 180 $^{\circ}$C and Si/Al=20, for 48h comparing with ZSM-5 commercial. It was observed that the signal with a chemical shift at around 53-55 ppm corresponds to the tetrahedral coordinated of Al atoms in the framework. While octahedral coordinated of Al atoms with extra-framework at about 0 ppm were not observed. It confirmed that the Al source occurred in the framework of synthesized ZSM-5/silica fibers.

From the results, it can conclude that ZSM-5/silica fibers synthesized under the hydrothermal conditions of pH 9 at 180 $^{\circ}$C for 48 h showed the good dispersion of ZSM-5 on silica fibers and still maintained the properties of fibrous material. The increasing of Si/Al ratio also increase the acidity of ZSM-5/silica fibers that the Al content played important role to the catalytic properties thus it should be considered in the LPG synthesis process.

4.2.4 The characterization of Pd-ZSM-5/silica fibers

The 0.1wt.% of Pd was loaded onto the ZSM-5/silica fibers by impregnation method to improve the hydrogen spilled-over and prohibited the coke formation on the surface of ZSM-5/silica fibers during LPG synthesis process. The components of Pd and ZSM-5/silica fibers was measured by EDX technique as shown in Table 4.5. The results showed that the low proportion of Pd metal loading on ZSM-5/silica fibers was 0.13% that closed to the desired loading.
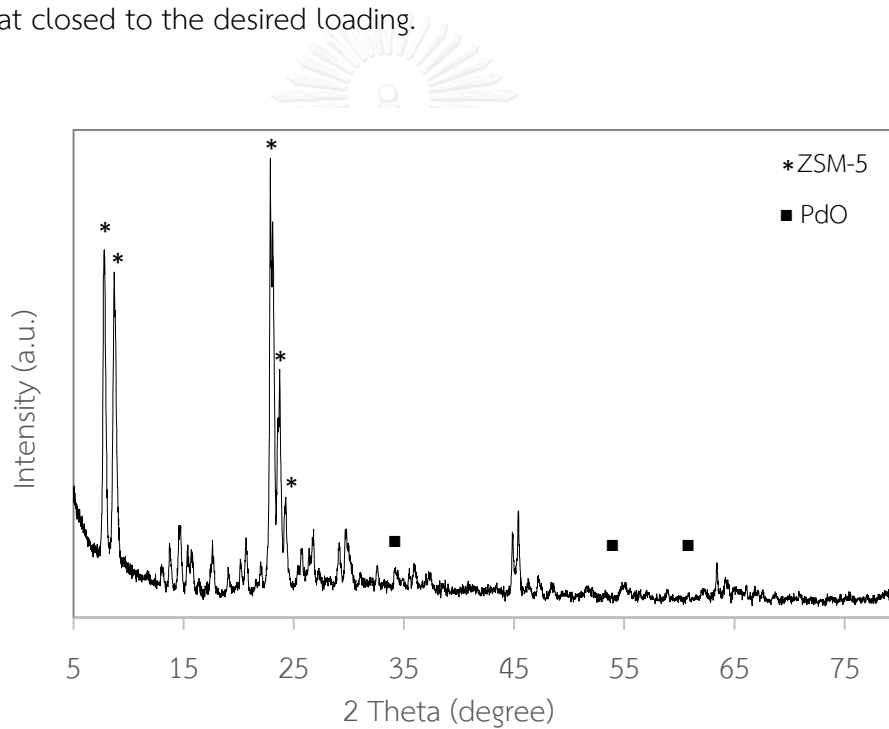
Figure 4.14 XRD patterns of Pd-ZSM-5/silica fibers

Table 4.5 Components of Pd on ZSM-5/silica fibers catalysts measured by EDX

Catalysts	%Component (wt.)			
	Si	Al	O	Pd
Pd-ZSM-5/silica fibers	87.1	4.7	8.07	0.13

In Figure 4.14, it showed the XRD pattern of Pd loaded on ZSM-5/silica fibers. The characteristic peak of palladium oxide was not observed because a very low palladium content was loaded onto ZSM-5/silica fibers.

4.3 **Catalyst characterization**

The effect of promoter addition with ZrO_2 and Al_2O_3 was studied by comparing with Cu/ZnO (CZ) based catalyst as non-addition promoter. In this section, The CZ and CZZA catalyst were characterized by EDX to measure element components and using XRD to study the crystal structure and crystallite size of metallic, then the reduction behavior was studied by temperature reduction program (TPR). The influence of addition promoters (Al_2O_3 and ZrO_2) comparing with conventional Cu/ZnO catalyst (CZ) were also studied.

4.3.1 Catalyst characterization by EDX

The components of CZ and CZZA catalysts were measured by EDX technique as shown in table 4.6. The results showed that showed the metallic ratio of Cu/ZnO catalyst indicating the proportion of CuO:ZnO nearly approximated with desired ratio at 2:1 more than Cu/ZnO-ZrO_2-Al_2O_3 catalyst. A more using of precursors were hardly controlled the concentration during the precipitated process so the component proportional of prepared catalysts was diverged from desired ratio.

Table 4.6 Components of CuO, ZnO, ZrO$_2$ and Al$_2$O$_3$ of CZ and CZZA catalysts measured by EDX

Catalysts	%Component (wt.)			
	CuO	ZnO	ZrO$_2$	Al$_2$O$_3$
Cu/ZnO (CZ)	68.72	32.18	-	-
Cu/ZnO-ZrO$_2$-Al$_2$O$_3$ (CZZA)	39.99	30.79	19.84	9.38

4.3.2 Catalyst characterization by XRD

The XRD patterns in Figure 4.15 showed the signal of CZ and CZZA catalyst with the ratio of CuO:ZnO of 2:1. The promoter addition of ZrO$_2$ and Al$_2$O$_3$ led to dramatically decrease the peak intensity of CuO locating at 2θ of 35.5, 38.8 and 48.7 degree comparing with non-promoter addition. The crystallite size of CuO was reduced from 366.7 to 105.2 Å measuring at 35.5 $^\circ$ and the characteristic peaks of ZnO at 2θ of 31.7, 34.3, 36.2, 47.5 and 56.5 degree were not observed. Because the addition of zirconium oxide metallic encouraged to decrease the metallic size and alumina also improved the metallic dispersion.
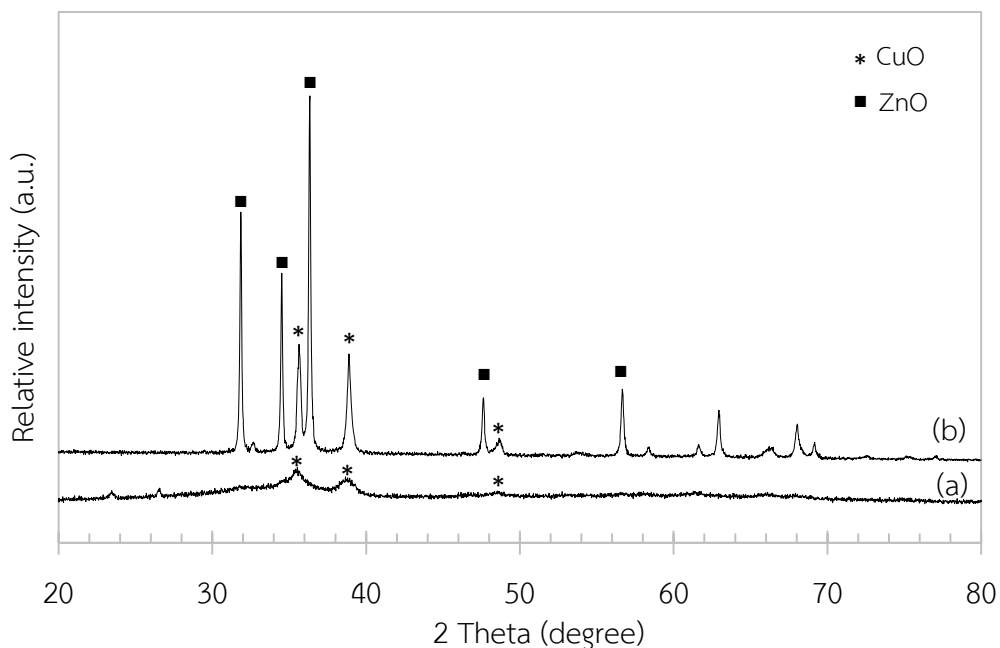
Figure 4.15 XRD patterns of (a) Cu/ZnO catalyst and (b) Cu/ZnO-ZrO$_2$-Al$_2$O$_3$ catalyst

4.3.3 Catalyst characterization by TPR

H$_2$-TPR profiles of CZ and CZZA catalyst were shown in Figure 4.16. From the results, it was observed the individual peaks assigned to the stepwise reduction of surface dispersed CuO species; Cu^{2+} $\longrightarrow$ Cu$^+$ $\longrightarrow$ Cu^0. The first peak at lower temperature assigned to the reduction of Cu^{2+} to Cu$^+$ illustrating in small shoulder peak. The second peak at higher temperature indicated the reduction of Cu$^+$ to Cu^0. The promoter addition of ZrO$_2$ and Al$_2$O$_3$ in Cu/ZnO catalyst tend to decrease the reduction temperature of CuO species from 285 $^\circ$C to 249 $^\circ$C as shown in Table 4.7 because the effect of Cu-O-Zr bounding is promoter oxide to redox chemistry of Cu and also enhanced the hydrogen consumption on catalyst surface that higher than Cu/ZnO catalyst with non-promoter resulting to increase a more active site to react

with feed gas over the surface at lower reaction temperature corresponding to the

smaller crystallite size from XRD results.
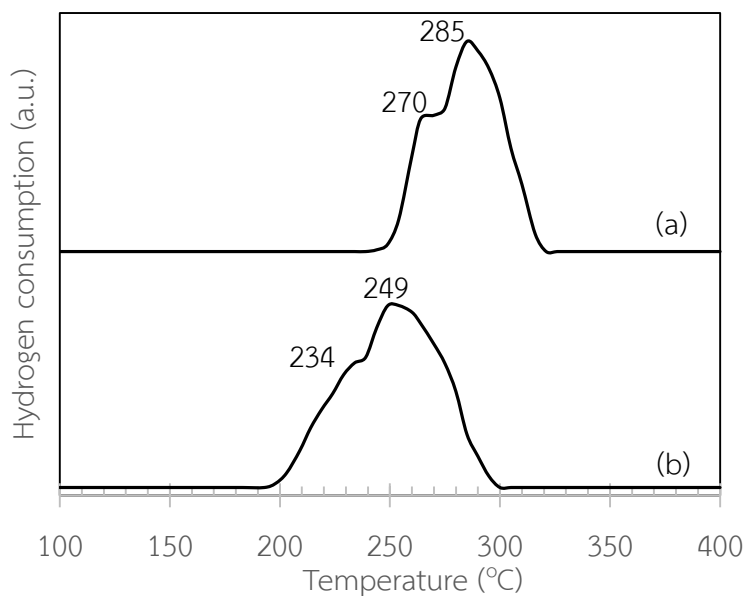
Figure 4.16 H_2-TPR profile of (a) Cu/ZnO catalyst and (b) Cu/ZnO-ZrO$_2$-Al$_2$O$_3$ catalyst

Table 4.7 Reduction temperature and %reduction of Cu/ZnO and Cu/ZnO-ZrO$_2$-Al$_2$O$_3$
catalyst measured by TPR

Type of catalyst	Reduction temperature ($^{\circ}$C)		% Reduction
	1st	2nd	
Cu/ZnO (CZ)	270	285	63.24
Cu/ZnO-ZrO$_2$-Al$_2$O$_3$ (CZZA)	234	249	68.63

4.4 **Catalytic activity test for LPG synthesis process**

4.4.1 The catalytic activity of CZ and CZZA catalyst

The catalytic activity test of Cu/ZnO (CZ) catalyst comparing with Cu/ZnO-ZrO$_2$-

Al$_2$O$_3$ (CZZA) was investigated by LPG synthesis reaction which both catalysts were

mixed with Pd-ZSM-5/silica fibers in weight ratio of 1:1 under the reaction condition of 260 $^\circ$C, 2 MPa and mole ratio of H_2/CO = 2, with W/F = 20 g cat h/mol. In Figure 4.17, it showed the comparison of CO conversion between CZ and CZZA catalyst. From the result, the CZZA catalyst provided the CO conversion at around 19% that higher than the CO conversion of CZ catalyst (approximately 10%). After 3h of operation, the CZZA catalyst exhibited a more stable of CO conversion than the CZ catalyst tended to decrease with the time.
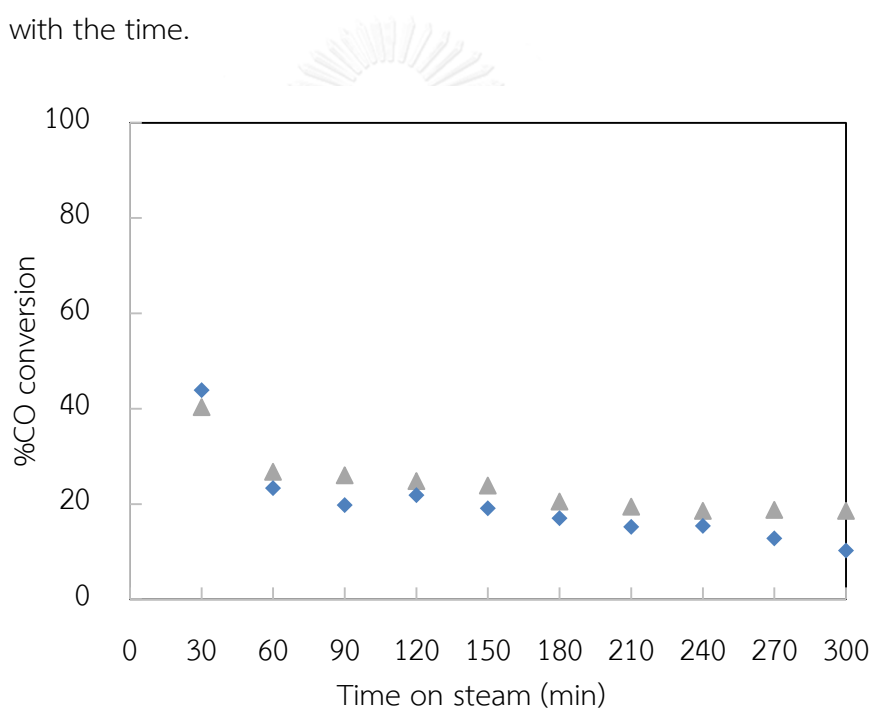
Figure 4.17 CO conversion (%) of (◆) mixed Cu/ZnO (CZ) and Pd-ZSM-5/silica fibers catalyst comparing with (▲) mixed Cu/ZnO-ZrO$_2$-Al$_2$O$_3$ (CZZA) and Pd-ZSM-5/silica fibers under the reaction condition of 260 $^\circ$C, 2 MPa and mole ratio of H_2/CO = 2, with W/F = 20 g cat h/mol.

The promoter addition of ZrO_2 and Al_2O_3 in CZZA catalyst help to retard the sintering of Cu active component. This results confirmed that the addition of ZrO_2 and Al_2O_3 promoters improved the CO conversion and the durability of catalyst activity.

So, the CZZA catalyst was selected for using as methanol synthesis catalyst mixing with Pd-ZSM-5/silica fibers for LPG synthesis.

4.4.2 The comparison of catalyst form

The catalytic performance of catalyst form was studied by comparing of mixed CZZA and Pd-ZSM-5/silica fibers with the mixed CZZA and Pd-ZSM-5 power under the reaction condition of $260 \,^{\circ}C$ and mole ratio of $H_2/CO = 2$, with W/F = 20 g cat h/mol. The mixed CZZA and Pd-ZSM-5/silica fibers catalyst provided a higher CO conversion, hydrocarbon yields and LPG selectivity. While the mixed CZZA and Pd-ZSM-5 powder catalyst provided the CO conversion and LPG selectivity only 18% and 38%, respectively.
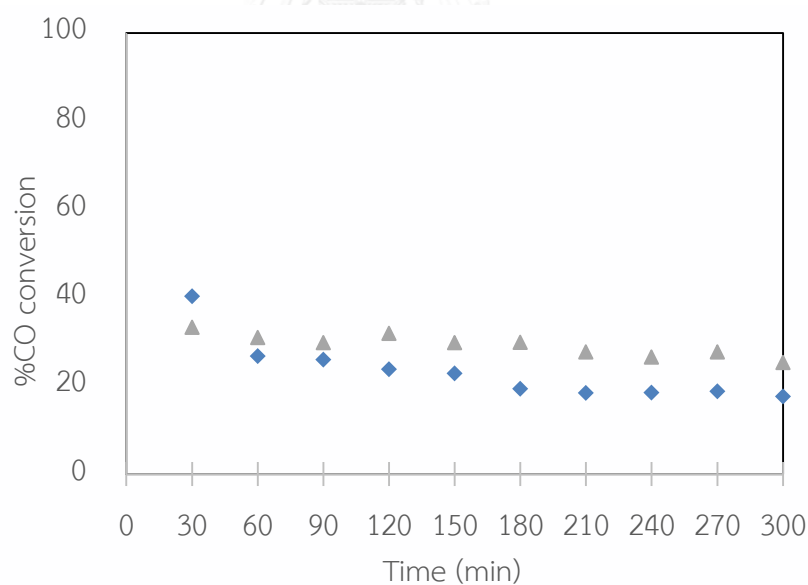
Figure 4.18 CO conversion (%) of (♦) mixed CZZA and Pd-ZSM-5 powder catalyst and (▲) mixed CZZA and Pd-ZSM-5/silica fibers under the reaction condition of $260 \,^{\circ}C$ and mole ratio of $H_2/CO = 2$, with W/F = 20 g cat h/mol

Because the properties of fibrous form catalyst had a low mass flow resistance and generated low pressure drop. In addition, it could improve the contract time of reactant over catalyst surface and reduced mass transfer limitation. So that, these phenomena would improve the CO conversion and LPG selectivity.

Table 4.8 Result of LPG synthesis from syngas over mixed CZZA and Pd-ZSM-5 powder catalyst comparing with mixed CZZA and Pd-ZSM-5/silica fibers under the reaction condition of 260 °C and mole ratio of H_2/CO = 2, with W/F = 20 g cat h/mol.

Catalysts	CZZA+ Pd-ZSM-5 powder	CZZA+ Pd-ZSM-5/silica fibers
CO conversion (%)	17.6	27.7
LPG selectivity (%)	38.4	56.3
Product yield (%CO feed)		
Hydrocarbon	15.12	20.24
CO_2	2.48	7.49
DME	-	-
Space-time yield of C_3+C_4 (mmol/h)	0.032	0.036
Hydrocarbon distribution (C%)		
C_1	1.8	8.1
C_2	3.5	10.7
C_3	8.6	35.8
C_4	60.3	41.3
C_5	24.8	4.1
C_6	1.0	-
C_3+C_4	68.9	77.1

4.4.3 The effect of reaction pressures

The influence of reaction pressures were investigated by various operating pressures of 1, 2 and 3 MPa by using the mixed catalyst of CZZA and Pd-ZSM-5/silica fibers (Si/Al=20) as a hybrid catalyst in weight ratio of 1:1, under the reaction condition of 260 $^{\circ}$C and mole ratio of H_2/CO = 2, with W/F = 20 g cat h/mol. Figure 4.19 showed the CO conversion of mixed CZZA and Pd-ZSM-5/silica fibers catalyst. The CO conversion and hydrocarbon yield tend to increase with increasing reaction pressure from 1 to 3 MPa while LPG selectivity dropped to 45% at 3MPa.
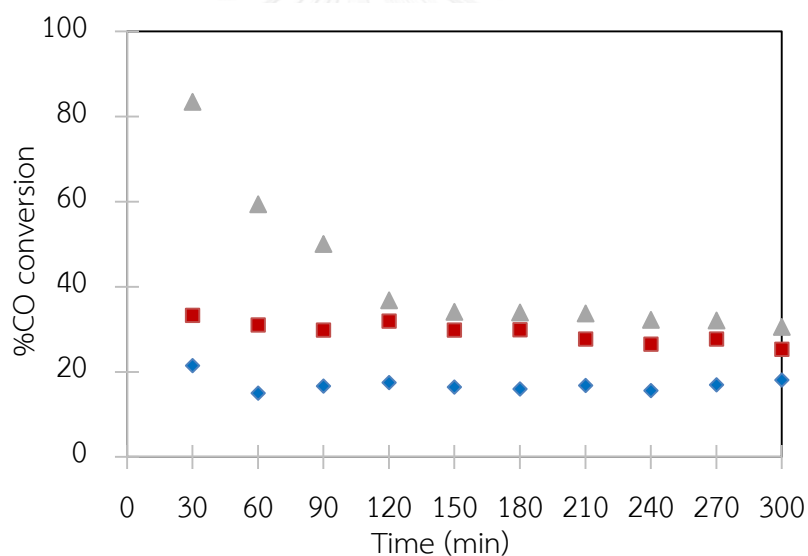
Figure 4.19 CO conversion (%) of mixed CZZA and Pd-ZSM-5/silica fibers with different reaction pressures at (◆) 1 MPa, (■) 2 MPa and (▲) 3MPa by using the mixed catalyst of CZZA and Pd-ZSM-5/silica fibers (Si/Al=20) as a hybrid catalyst in weight ratio of 1:1, under the reaction condition of 260 $^{\circ}$C and mole ratio of H_2/CO = 2, with W/F = 20 g cat h/mol

The reaction pressure of 1 MPa provided the lowest CO conversion of 16% while the reaction pressures at 2 and 3 MPa exhibited a slightly increase of CO conversions at around 27.7% and 30.6 %, respectively. However, at the reaction

pressure of 3 MPa, selectivity of C_1 and C_2 decreased and selectivity of heavier hydrocarbon (C_5 and C_6) increased as shown in table 4.9. Because at high reaction pressure causing to promote the possibly of hydrocarbon chain growth from lighten hydrocarbon to be heavy hydrocarbon product. Therefore, the suitable reaction pressure to obtain a high LPG selectivity and high CO conversion was 2 MPa.

Table 4.9 Result of LPG synthesis from syngas over mixed of CZZA and Pd-ZSM-5/silica fibers with different reaction pressures by using the mixed catalyst of CZZA and Pd-ZSM-5/silica fibers (Si/Al=20) as a hybrid catalyst in weight ratio of 1:1, under the reaction condition of 260 $^{\circ}$C and mole ratio of H_2/CO = 2, with W/F = 20 g cat h/mol

Pressure (MPa)	1	2	3
CO conversion (%)	16.0	27.7	30.6
LPG selectivity (%)	54.1	56.3	45.0
Product yield (%CO feed)			
Hydrocarbon	13.33	20.24	23.48
CO_2	2.67	7.49	7.12
DME	-	-	-
Space-time yield of C_3+C_4 (mmol/h)	0.011	0.036	0.055
Hydrocarbon distribution (C%)			
C_1	7.6	8.1	4.8
C_2	11.5	10.7	11.7
C_3	36.9	35.8	26.5
C_4	38.0	41.3	32.2
C_5	5.9	4.1	21.9
C_6	-	-	2.9
C_3+C_4	74.9	77.1	58.7

4.4.4   The effect of reaction temperatures

The effect of reaction temperature was investigated at various temperature of 260, 270 and 280 °C by using the mixed catalyst of CZZA and Pd-ZSM-5/silica fibers (Si/Al=20) as a hybrid catalyst in weight ratio of 1:1, under the reaction condition of 2 MPa and mole ratio of $H_2/CO = 2$, with W/F = 20 g cat h/mol. From the %CO conversion in Figure 4.20, it showed the CO conversion had a slightly increased with increased the reaction temperature from 260 to 280 °C. At the temperature of 260 °C, it provided the highest LPG selectivity at around 56.3%. At the temperature of 270 and 280 °C, it provides the slightly increased of CO conversion at around 32.2 to 34.2%, respectively.
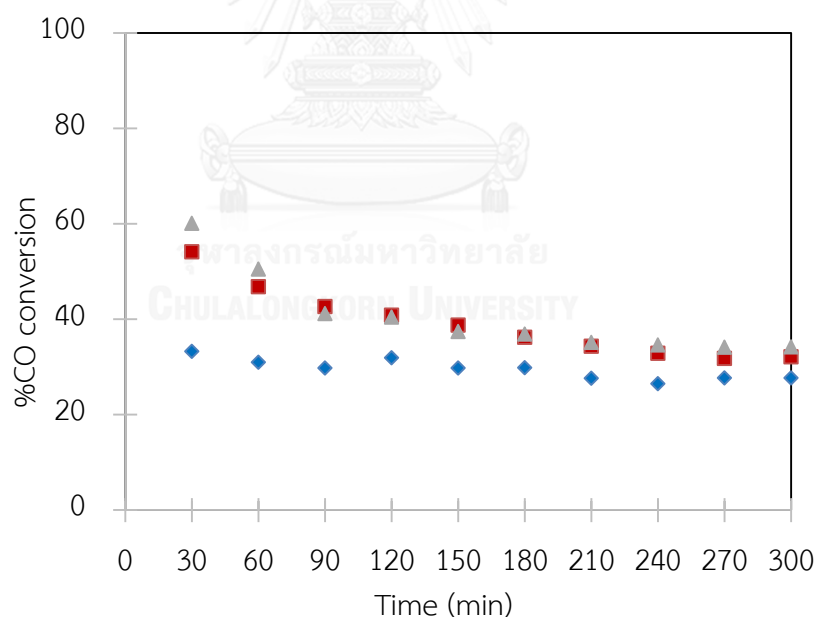
Figure 4.20 CO conversion (%) of mixed CZZA and Pd-ZSM-5/silica fibers with different reaction temperatures at (◆) 260 °C, (■) 270 °C and (▲) 280 °C by using the mixed catalyst of CZZA and Pd-ZSM-5/silica fibers (Si/Al=20) in weight ratio of 1:1, under the reaction condition of 2 MPa and mole ratio of $H_2/CO = 2$, with W/F = 20 g cat h/mol.

Table 4.10 Result of LPG synthesis from syngas over mixed of CZZA and Pd-ZSM-5/silica fibers with different reaction pressure by using the mixed catalyst of CZZA and Pd-ZSM-5/silica fibers (Si/Al=20) in weight ratio of 1:1, under the reaction condition of 2 MPa and mole ratio of H_2/CO = 2, with W/F = 20 g cat h/mol.

Temperature ($^\circ$C)	260	270	280
CO conversion (%)	27.7	32.2	34.2
LPG selectivity (%)	56.3	48.6	46.2
Product yield (%CO feed)			
Hydrocarbon	20.24	24.54	26.68
CO_2	7.49	7.62	7.48
DME	-	-	-
Space-time yield of C_3+C_4 (mmol/h)	0.036	0.055	0.042
Hydrocarbon distribution (C%)			
C_1	8.1	8.6	12.7
C_2	10.7	21.0	20.3
C_3	35.8	30.0	30.9
C_4	41.3	33.1	28.3
C_5	4.1	7.3	7.8
C_6	-	-	-
C_3+C_4	77.1	63.1	59.2

Increasing of reaction temperature from 260 to 280 $^\circ$C affected to increase the %CO conversion and hydrocarbon yield. The increasing trends become slow after 270 $^\circ$C while the %LPG selectivity slightly decreased because at the high reaction temperature range (270-280 $^\circ$C), it started to reduce rate of methanol formation for

hydrocarbon synthesis from synthesis gas. From the product hydrocarbon distribution as shown in Table 4.10, the selectivity of C_1–C_3 was increased and selectivity of C_4–C_6 decreased with increase in reaction temperature, this is due to high dehydration and olefin hydrogenation ability of Pd-ZSM-5/silica fibers at higher temperature causing to promote the cracking of heavy hydrocarbon product to be lighten hydrocarbon. From the results consisting of the factors of conversion, LPG selectivity, and hydrocarbon distribution, it is supposed that at 260 °C is the suitable reaction temperature for LPG synthesis from syngas over mixed CZZA and Pd–ZSM-5/silica fibers catalyst.

4.4.5 The effect weight catalyst to feed flow rate ratio (W/F)

The influence of weight catalyst to feed flow rate (W/F ratio) was studied with various the W/F ratio of 10, 20 and 40 g cat h/mol by using the mixed catalyst of CZZA and Pd-ZSM-5/silica fibers (Si/Al=20) as a hybrid catalyst in weight ratio of 1:1, under the reaction condition at 260 °C of 2 MPa and mole ratio of H_2/CO=2. At W/F ratio of 40, it provided the highest CO conversion and LPG selectivity at 34% and 66 %, respectively. While the space-time yield of C_3+C_4 at W/F ratio of 40 slightly less than W/F ratio of 20. From this results, it showed the CO conversion, LPG selectivity and hydrocarbon yield (table 4.11) increased with W/F increased. Because the contact time of feed gas with catalyst was enhanced with increasing of W/F ratio and formed a more C_3-C_4 hydrocarbon product further the cracking to lighten hydrocarbon. The low W/F ratio resulting in a low CO conversion, hydrocarbon yield and LPG selectivity was

affected to reduce the formation rate of methanol synthesis from synthesis gas, which is the rate-determining step in the process of LPG synthesis to hydrocarbons. While at the high W/F ratio, the gas space velocity will decrease causing to occur the carbon chain growth, which will increase the larger hydrocarbon product. Therefore, the suitable W/F ratio to obtain a high CO conversion and LPG selectivity was 40 g h/mol.

Table 4.11 Result of LPG synthesis from syngas over mixed of CZZA and Pd-ZSM-5/silica fibers with different weight catalyst to feed flow rate under the reaction condition at $260\,^{\circ}C$ of 2 MPa and mole ratio of $H_2/CO=2$

W/F ratio (g h/mol)	10	20	40
CO conversion (%)	8.8	27.7	33.5
LPG selectivity (%)	25.3	56.3	66.1
Product yield (%CO feed)			
Hydrocarbon	8.0	20.24	26.93
CO_2	0.8	7.49	6.55
DME	-	-	-
Space-time yield of C_3+C_4 (mmol/h)	0.001	0.036	0.033
Hydrocarbon distribution (C%)			
C_1	57.7	8.1	5.8
C_2	12.8	10.7	10.3
C_3	7.2	35.8	40.6
C_4	22.3	41.3	37.0
C_5	-	4.1	5.1
C_6	-	-	1.2
C_3+C_4	29.5	77.1	77.6
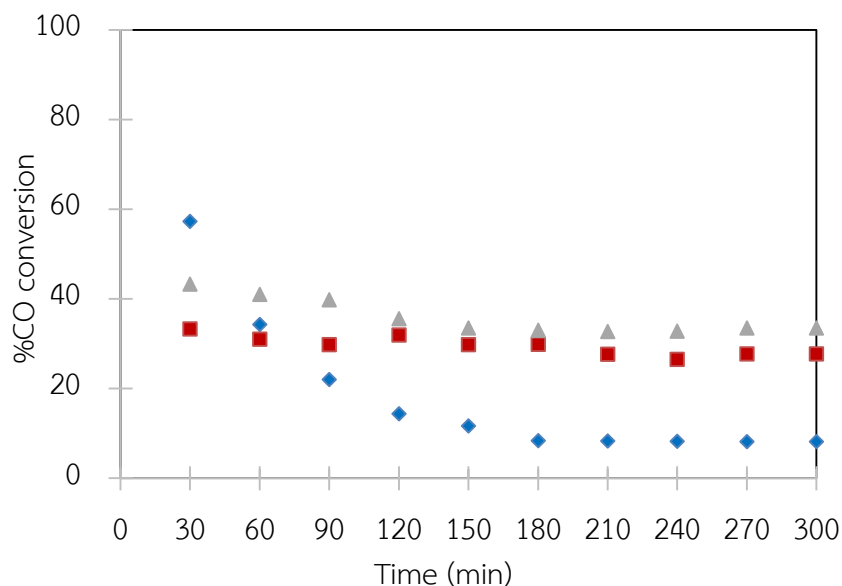
Figure 4.21 CO conversion (%) of mixed CZZA and Pd-ZSM-5/silica fibers with different weight catalyst to feed flow rate of (♦)10 g.h/mol, (■) 20 g.h/mol and (▲) 40 g.h/mol under the reaction condition at 260 °C of 2 MPa and mole ratio of $H_2/CO=2$

4.4.6 The effect of Si/Al ratios

The influence of Si/Al ratio was investigated at various the ratio of 20, 40 and 60 by using the mixed catalyst of CZZA and Pd-ZSM-5/silica fibers as a hybrid catalyst in weight ratio of 1:1, under the reaction condition at 260 °C of 2 MPa and mole ratio of $H_2/CO=2$, with W/F = 40 g cat h/mol. From the results, it indicated that CO conversion, hydrocarbon yields and LPG selectivity increase with increasing of Si/Al ratio from 20 to 40. At the Si/Al ratio of 20, it provided lowest CO conversion due to quickly deactivation exhibiting a low catalytic performance, and the major products at this ratio were light hydrocarbon as C_1 and C_2 because the higher acidity (total acid amount of 0.164 mmol/g) promoted the severe cracking reaction of long chain

hydrocarbon to be lighten hydrocarbon resulting to low LPG selectivity. The heavier

hydrocarbon product (C_{5+}) was obtained by Si/Al ratio of 60 and presented the lowest

CO conversion at around 37% because it had a low acidity led to decrease the cracking

reaction of long chain hydrocarbon to light hydrocarbon. While the ratio at 40 provided

the highest CO conversion and LPG selectivity at around 60% and 79%, respectively

because the suitable acidity of Pd-ZSM-5/silica fibers, which are mainly related to Al

component enhancing the dehydration ability from MeOH/DME to hydrocarbons, and

further the catalytic activity of catalysts increase. So that, the Si/Al ratio of 40 was

suitable ratio to provide the highest CO conversion, hydrocarbon yield and LPG

selectivity.
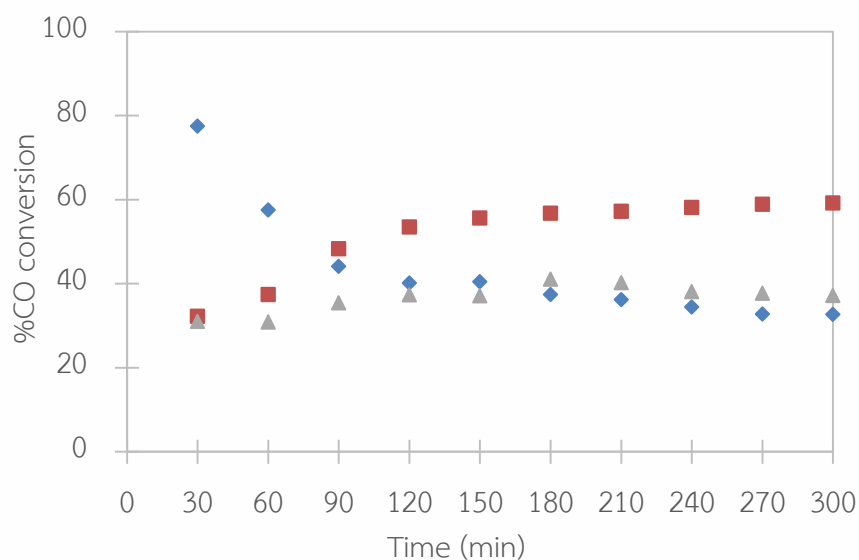
Figure 4.22 CO conversion (%) of mixed CZZA and Pd-ZSM-5/silica fibers with different Si/Al ratios of (◆) 20, (■) 40 and (▲) 60 under the reaction condition at 260 °C of 2 MPa and mole ratio of H_2/CO=2, with W/F = 40 g cat h/mol.

Table 4.12 Result of LPG synthesis from syngas over mixed of CZZA and Pd-ZSM-5/silica fibers with different Si/Al ratios under the reaction condition at 260 $^\circ$C of 2 MPa and mole ratio of H_2/CO=2, with W/F = 40 g cat h/mol.

W/F ratio (g h/mol)	20	40	60
CO conversion (%)	33.5	59.3	37.2
LPG selectivity (%)	66.1	78.9	46.2
Product yield (%CO feed)			
Hydrocarbon	26.93	56.02	34.97
CO_2	6.55	3.23	2.27
DME	-	-	-
Space-time yield of C_3+C_4 (mmol/h)	0.033	0.045	0.012
Hydrocarbon distribution (C%)			
C_1	5.8	5.1	3.5
C_2	10.3	8.4	7.7
C_3	40.6	34.1	16.1
C_4	37.0	47.6	33.1
C_5	5.1	4.8	25.1
C_6	1.2	2.3	14.6
C_3+C_4	77.6	81.7	49.1

CHAPTER V

Conclusion and recommendation

5.1 Conclusion

The ZSM-5 on silica fiber was achieved by electrospinning technique followed by hydrothermal process. The core structure as silica fiber was prepared by sol-gel method assisted electrospinning technique with needle size 0.25 mm, TCD 15 cm, applied a high voltage of 20 kV and spinning rate of 10 mL/h. The prepared silica fibers had average diameter of 0.68 μm with low surface area of 3.8 m²/g. ZSM-5 deposition on silica fibers was performed at pH of solution at pH 9 under the hydrothermal condition of 180 $^\circ$C for 48 h with high surface area of 273 m²/g. The crystal structure of all samples were confirmed by XRD technique, the XRD patterns indicated two characteristic peaks at 2 theta between 7-10 and 22-25 corresponding to be the MFI structure. The crystallization times is significantly parameter to increase surface area of ZSM-5/silica fibers. The crystal size of ZSM-5 on silica fibers were decreased by increase pH of solution from 8 to 10. The increasing of Si/Al ratio from 20 to 60 decrease the total acid amount of samples. The catalytic properties of ZSM-5/silica fibers were investigated by LPG synthesis reaction by using the hybrid catalyst consisting of Cu/ZnO-ZrO$_2$-Al$_2$O$_3$ and Pd-ZSM-5/silica fibers in the weight ratio of 1:1. These catalysts were characterized by SEM, EDX, XRD, TPD and TPR prior catalytic testing. The EDX can confirm that the Pd-ZSM-5/silica fibers catalyst contained Si, Al,

O and Pd element. The XRD results revealed that addition promoter of ZrO_2 and Al_2O_3 can reduce the crystallite size of CuO from 366.7 to 105.2 Å calculating from scherrer equation. The TPR profiles at 220 – 300 $^{\circ}$C indicated the reduction of $Cu^{2+} \longrightarrow Cu^+ \longrightarrow$ Cu^0. The promoter addition of ZrO_2 and Al_2O_3 in Cu/ZnO catalyst decreased the reduction temperature of CuO species from 285 $^{\circ}$C to 250 $^{\circ}$C due to Cu-O-Zr bounding as promoter oxide to improve redox chemistry of Cu. The highest CO conversion and LPG selectivity were obtained under the operating conditions of 260 $^{\circ}$C, 2 MPa with W/F ratio of 40 g cat h/mol by using the mixed catalyst of CZZA and Pd-ZSM-5/silica fibers with Si/Al ratio of 40. It provided the CO conversion and LPG selectivity of 60% and 79%, respectively.

5.2 Recommendation

Although ZSM-5 can be deposited on silica fibers by sol-gel method assisted electrospinning technique followed by hydrothermal process but this technique required to control drying of the gel on fibers. Excessive gel dryness affected to hardly coat of ZSM-5 on silica fibers. Moreover, adding of the gel also caused to changing the chemical composition. Therefore ZSM-5 deposition on silica fibers without gel coating should be developed by adjusting silica fiber loading, Si /Al ratio, aging time, H_2O content and sequence of adding.

REFERENCES

1.   Ma, X., et al., *Synthesis of LPG via DME from syngas in two-stage reaction system.* Fuel Processing Technology, 2013. **109**(0): p. 1-6.

2.   Ma, X., et al., *Direct synthesis of LPG from syngas derived from air-POM.* Fuel, 2011. **90**(5): p. 2051-2054.

3.   Ge, Q., et al., *High performance Cu–ZnO/Pd-β catalysts for syngas to LPG.* Catalysis Communications, 2008. **9**(2): p. 256-261.

4.   Zhang, Q., et al., *Synthesis of LPG from synthesis gas.* Fuel Processing Technology, 2004. **85**(8–10): p. 1139-1150.

5.   Jin, Y., et al., *Synthesis of liquefied petroleum gas via methanol/dimethyl ether from natural gas.* Fuel processing technology, 2004. **85**(8): p. 1151-1164.

6.   Ivanova, S., et al., *ZSM-5 coatings on β-SiC monoliths: possible new structured catalyst for the methanol-to-olefins process.* The Journal of Physical Chemistry C, 2007. **111**(11): p. 4368-4374.

7.   Jansen, J.C., et al., *Zeolitic coatings and their potential use in catalysis.* Microporous and Mesoporous Materials, 1998. **21**(4–6): p. 213-226.

8.   Sang, S., et al., *Difference of ZSM-5 zeolites synthesized with various templates.* Catalysis Today, 2004. **93–95**(0): p. 729-734.

9.   Georgiev, D., et al. *Synthetic zeolites–Structure, classification, current trends in zeolite synthesis.* in *Review."Economics and Society development on the Base of Knowledge": Int. Sci. Conf. VII, Stara Zagora.* 2009.

10.   Van der Gaag, F.J., *ZSM-5 type zeolites: Synthesis and use in gasphase reactions with ammonia*, in *Applied Sciences.* 1987, Technische Universiteit Delft: Holland.

11.   Byrappa, K. and M. Yoshimura, *Handbook of hydrothermal technology.* 2012: William Andrew.

12.   Singh, R. and P.K. Dutta, *MFI: a case study of zeolite synthesis.* Handbook of Zeolite Science and Technology, 2003: p. 21-63.

13. Cundy, C.S. and P.A. Cox, *The hydrothermal synthesis of zeolites: Precursors, intermediates and reaction mechanism.* Microporous and Mesoporous Materials, 2005. **82**(1–2): p. 1-78.

14. Cundy, C.S., J.O. Forrest, and R.J. Plaisted, *Some observations on the preparation and properties of colloidal silicalites. Part I: synthesis of colloidal silicalite-1 and titanosilicalite-1 (TS-1).* Microporous and Mesoporous Materials, 2003. **66**(2–3): p. 143-156.

15. Selvin, R., et al., *Effect of Aging on the Precursor Sol for the Synthesis of Nanocrystalline ZSM-5.* Synthesis and Reactivity in Inorganic, Metal-Organic, and Nano-Metal Chemistry, 2011. **41**(8): p. 1028-1032.

16. Cejka, J., et al., *Introduction to Zeolite Molecular Sieves*. Vol. 168. 2007: Elsevier.

17. Wakihara, T. and T. Okubo, *Hydrothermal synthesis and characterization of zeolites.* Chemistry Letters, 2005. **34**(3): p. 276-281.

18. Karimi, R., et al., *Studies of the effect of synthesis parameters on ZSM-5 nanocrystalline material during template-hydrothermal synthesis in the presence of chelating agent.* Powder Technology, 2012. **229**(0): p. 229-236.

19. Krissanasaeranee, M., et al., *Preparation of Ultra‑Fine Silica Fibers Using Electrospun Poly (Vinyl Alcohol)/Silatrane Composite Fibers as Precursor.* Journal of the American Ceramic Society, 2008. **91**(9): p. 2830-2835.

20. Taek Jung, K., et al., *Synthesis of mesoporous silica fiber using spinning method.* Journal of Non-Crystalline Solids, 2002. **298**(2–3): p. 193-201.

21. Attia, S., *Review on Sol—Gel Derived Coatings: Process, Techniques and Optical Applications.* 材料科学技术学报: 英文版, 2002. **18**(3): p. 211-218.

22. Miao, J., et al., *Electrospinning of Nanomaterials and Applications in Electronic Components and Devices.* Journal of Nanoscience and Nanotechnology, 2010. **10**(9): p. 5507-5519.

23. Huang, Z.-M., et al., *A review on polymer nanofibers by electrospinning and their applications in nanocomposites.* Composites Science and Technology, 2003. **63**(15): p. 2223-2253.

24. Pham, Q.P., U. Sharma, and A.G. Mikos, *Electrospinning of polymeric nanofibers for tissue engineering applications: a review.* Tissue engineering, 2006. **12**(5): p. 1197-1211.

25. Frenot, A. and I.S. Chronakis, *Polymer nanofibers assembled by electrospinning.* Current Opinion in Colloid & Interface Science, 2003. **8**(1): p. 64-75.

26. Sakai, S., K. Kawakami, and M. Taya, *Controlling the Diameters of Silica Nanofibers Obtained by Sol–Gel/Electrospinning Methods.* Journal of chemical engineering of Japan, 2012. **45**(6): p. 436-440.

27. Pirzada, T., et al., *Hybrid silica–PVA nanofibers via sol–gel electrospinning.* Langmuir, 2012. **28**(13): p. 5834-5844.

28. Liu, F., et al., *Effect of Processing Variables on the Morphology of Electrospun Poly [(lactic acid)‐co‐(glycolic acid)] Nanofibers.* Macromolecular materials and engineering, 2009. **294**(10): p. 666-672.

29. Van Der Laan, G.P. and A. Beenackers, *Kinetics and selectivity of the Fischer–Tropsch synthesis: a literature review.* Catalysis Reviews, 1999. **41**(3-4): p. 255-318.

30. Totten, G.E., S. Westbrook, and R. Shah, *Fuels and lubricants handbook: technology, properties, performance, and testing.* Training, 2003. **2007**: p. 08-21.

31. Bosch, R. and U. Adler, *Automotive handbook.* 1996: Society of Automotive Engineers, US.

32. Qi, D.H., et al., *Combustion and exhaust emission characteristics of a compression ignition engine using liquefied petroleum gas–Diesel blended fuel.* Energy Conversion and Management, 2007. **48**(2): p. 500-509.

33. Zhang, C., et al., *A study on an electronically controlled liquefied petroleum gas-diesel dual-fuel automobile.* Proceedings of the Institution of Mechanical Engineers, Part D: Journal of Automobile Engineering, 2005. **219**(2): p. 207-213.

34. Behrens, M., et al., *The active site of methanol synthesis over Cu/ZnO/Al2O3 industrial catalysts.* Science, 2012. **336**(6083): p. 893-897.

35. Yoshihara, J. and C.T. Campbell, *Methanol Synthesis and Reverse Water–Gas Shift Kinetics over Cu(110) Model Catalysts: Structural Sensitivity.* Journal of Catalysis, 1996. **161**(2): p. 776-782.

36. Rasmussen, P.B., et al., *Dissociative adsorption of hydrogen on Cu(100) at low temperatures.* Surface Science, 1993. **287–288, Part 1**(0): p. 79-83.

37. Szanyi, J. and D.W. Goodman, *Methanol synthesis on a Cu (100) catalyst.* Catalysis letters, 1991. **10**(5-6): p. 383-390.

38. Spencer, M., *The role of zinc oxide in Cu/ZnO catalysts for methanol synthesis and the water–gas shift reaction.* Topics in Catalysis, 1999. **8**(3-4): p. 259-266.

39. Nakamura, J., et al., *A Surface Science Investigation of Methanol Synthesis over a Zn-Deposited Polycrystalline Cu Surface.* Journal of Catalysis, 1996. **160**(1): p. 65-75.

40. Burch, R., R.J. Chappell, and S.E. Golunski, *Synergy between copper and zinc oxide during methanol synthesis. Transfer of activating species.* Journal of the Chemical Society, Faraday Transactions 1: Physical Chemistry in Condensed Phases, 1989. **85**(10): p. 3569-3578.

41. Chuang, S.S., *Conversion of syngas to fuels*, in *Handbook of Climate Change Mitigation*. 2012, Springer. p. 1605-1621.

42. Yildiz, M. and A.N. Akin, *Deactivation of a Co-Precipitated Co/Al2O3 Catalyst.* Turkish Journal of Chemistry, 2007. **31**(5): p. 515-521.

43. Yang, G., et al., *Tandem catalytic synthesis of light isoparaffin from syngas via Fischer–Tropsch synthesis by newly developed core–shell-like zeolite capsule catalysts.* Catalysis Today, 2013. **215**(0): p. 29-35.

44. Yang, G., et al., *Preparation, characterization and reaction performance of H-ZSM-5/cobalt/silica capsule catalysts with different sizes for direct synthesis of isoparaffins.* Applied Catalysis A: General, 2007. **329**(0): p. 99-105.

45. Louis, B., et al., *Synthesis of structured filamentous zeolite materials via ZSM-5 coatings of glass fibrous supports.* Catalysis today, 2001. **69**(1): p. 365-370.

46. Van Vu, D., et al., *Catalytic activities and structures of silicalite-1/H-ZSM-5 zeolite composites.* Microporous and Mesoporous Materials, 2008. **115**(1): p. 106-112.

47. Choi, S.-S., et al., *Silica nanofibers from electrospinning/sol-gel process.* Journal of Materials Science Letters, 2003. **22**(12): p. 891-893.

48. Yodwanlop, P., *Preparation of Co/SiO$_2$ fiber by electrospinning technique for fischer-tropsch synthesis*, in *Chemical Technology*. 2010, Chulalongkorn: Thailand.

APPENDIX

Appendix A

Calculation for preparation of silica fibers

Molar ratio composition

1 TEOS: 2 EtOH: $2H_2O$: 0.0144 HCl

Starting from H_2O 3 ml

$$\therefore \text{mol } H_2O = 3 \text{ ml} \times \frac{1 \text{ g}}{1 \text{ ml}} \times \frac{1 \text{ mol}}{18 \text{ g}} = 0.1667 \text{ mol}$$

TEOS content (calculated from 100% of concentration)

$$= \frac{3 \text{ ml } H_2O}{18 \text{ g/mol } H_2O} \times \frac{1 \text{ g } H_2O}{1 \text{ ml } H_2O} \times \frac{1 \text{ mol TEOS}}{2 \text{ mol } H_2O} \times \frac{208.33 \text{ g TEOS}}{1 \text{ mol TEOS}} \times \frac{1 \text{ ml TEOS}}{0.94 \text{ g TEOS}}$$

= 18.02 ml

Ethanol content (calculated from 95% of concentration)

$$= \frac{3 \text{ ml } H_2O}{18 \text{ g/mol } H_2O} \times \frac{1 \text{ g } H_2O}{1 \text{ ml } H_2O} \times \frac{2 \text{ mol EtOH}}{2 \text{ mol } H_2O} \times \frac{46.07 \text{ g EtOH}}{1 \text{ mol EtOH}} \times \frac{1 \text{ ml TEOS}}{0.79 \text{ g TEOS}} \times \frac{1}{0.995}$$

= 9.77 ml

HCl content (calculated from 37 % of concentration)

$$= \frac{3 \text{ ml } H_2O}{18 \text{ g/mol } H_2O} \times \frac{1 \text{ g } H_2O}{1 \text{ ml } H_2O} \times \frac{0.0144 \text{ mol HCl}}{2 \text{ mol } H_2O} \times \frac{36.46 \text{ g HCl}}{1 \text{ mol HCl}} \times \frac{1 \text{ ml HCl}}{1.18 \text{ g HCl}} \times \frac{1}{0.37}$$

= 0.10 ml

Calculation for ZSM-5 synthesis

Molar ratio composition

1 TEOS: 0.25TPAOH: $0.025Al(NO_3)_3.9H_2O$: $80H_2O$. at Si/Al=40

Starting from H_2O 30 ml

$\therefore$ mol H_2O

$$= 30 \text{ ml} \times \frac{1 \text{ g}}{1 \text{ ml}} \times \frac{1 \text{ mol}}{18 \text{ g}} = 1.67 \text{ mol}$$

g of $Al(NO_3)_3.9H_2O$

$$= 0.0250 \text{ mol Al(NO}_3)_3.9H_2O \times \frac{375.134 \text{ g}}{1 \text{ mol}} \times \frac{30 \text{ ml H}_2O}{18 \text{ g/mol H}_2O} \times \frac{1 \text{ g H}_2O}{1 \text{ ml H}_2O} \times$$

$$\frac{1}{80 \text{ mol H}_2O}$$

$$= 0.1953 \text{ g}$$

TEOS content (calculated from 100% of concentration)

$$= \frac{30 \text{ ml H}_2O}{18 \text{ g/mol H}_2O} \times \frac{1 \text{ g H}_2O}{1 \text{ ml H}_2O} \times \frac{1 \text{ mol TEOS}}{80 \text{ mol H}_2O} \times \frac{208.33 \text{ g TEOS}}{1 \text{ mol TEOS}} \times \frac{1 \text{ ml TEOS}}{0.94 \text{ g TEOS}}$$

$$= 4.63 \text{ ml}$$

TPAOH content (calculated from 20.34 % of concentration)

$$= \frac{30 \text{ ml H}_2O}{18 \text{ g/mol H}_2O} \times \frac{1 \text{ g H}_2O}{1 \text{ ml H}_2O} \times \frac{0.25 \text{ mol TPAOH}}{80 \text{ mol H}_2O} \times \frac{203.37 \text{ g TPAOH}}{1 \text{ mol TPAOH}} \times \frac{1}{0.2034}$$

$$= 5.22 \text{ ml}$$

Calculation of Pd loading

Deposition of 10%wt Pd on ZSM-5/silica fibers by incipient wetness impregnation

Loading 0.1 wt.% of Pd into 0.5 g of ZSM-5 porous

ZSM-5/silica fibers 90 g compose of Pd 1.0 g

ZSM-5/silica fibers 5.0 g compose of Pd (1.0×5.0) ÷ 90 g = 0.0556 g

If require Pd 106.4 g, weight $Pd(NO_3)_2.2H_2O$ 266.46 g

If require Pd 0.0556 g, weight $Pd(NO_3)_2.2H_2O$ = (266.46×0.0556) ÷ 106.4 = 0.139 g

Pore volume from water drop test of ZSM-5/silica fibers = 0.264 ml/g

∴ If prepare 5 g of catalyst, the solution should be 0.264 × 5 = 1.32 ml

Calculation of %reduction

Catalyst: CZZA catalyst

Flow rate of H_2 =   30.00 ml/min from 5% H_2 balanced in in N_2

∴   Flow rate of H_2 =   0.05 x 30.00 ml/min

=   1.50 ml H_2 /min

Calculated mol of H$_2$ (real)

From $\qquad$ n $\quad$ = $\quad$ $\dfrac{Pv}{RT}$

Where $\qquad$ P $\quad$ = $\quad$ pressure (atm)

$\qquad$ v $\quad$ = $\quad$ volume (ml/min)

$\qquad$ R $\quad$ = $\quad$ 82.057 atm·ml/mol·K

$\qquad$ T $\quad$ = $\quad$ temperature (K)

Thus $\qquad$ mol H$_2$ /min $\quad$ = $\quad$ $\dfrac{1\ atm \times 1.50\ ml/min}{82.057\ atm \cdot \dfrac{ml}{mol \cdot K} \times 298\ K}$

$\qquad\qquad$ = $\quad$ 6.1342 × 10^{-5} mol H$_2$ /min

Area of H$_2$ before reduced $\quad$ = $\quad$ 89233.6 area/min

$\qquad\qquad$ = $\quad$ 6.6964 × 10^{-5} mol H$_2$ /min

Area of H$_2$ after reduced $\quad$ = $\quad$ 864341.85 area/min

$\qquad$ mol H$_2$ /min $\quad$ = $\quad$

$$\dfrac{864341.85\ area\ /min \times (6.6964 \times 10^{-5})\ mol\ H_2/min}{89233.6\ area/min}$$

$\qquad\qquad$ = $\quad$ 6.486 × 10^{-4} mol H$_2$ /min (real)

Weight 60% of copper on 0.1 g of catalyst

Molecular weight of Cu = 63.5 g/mol

60 % by weight of copper in the 0.1 g of catalyst

= (0.1 × 60) ÷ 100 = 0.06 g

= 0.06 ÷ 63.5 = 0.000945 mol

From equation $\qquad$ CuO $\quad$ + $\quad$ H$_2$ $\quad$ → $\quad$ Cu $\quad$ + $\quad$ H$_2$O

Ratio $\qquad\qquad$ 1 $\qquad$: 1 $\qquad$: 1 $\qquad$: 1

$\qquad\qquad$ $\dfrac{0.000945}{1}$ $\quad$: $\quad$ $\dfrac{0.000945}{1}$ $\quad$: $\quad$ $\dfrac{0.000945}{1}$ $\quad$: $\quad$ $\dfrac{0.000945}{1}$

mol H$_2$ (Theory) =   0.000945 mol

% reduction   =   [mol H$_2$ (real)/ mol H$_2$ (theory)] ×100

           =   [(6.486 × 10^{-4}) ÷ (9.45 × 10^{-4})] ×100

=   68.63 %

Calculation of CO conversion, LPG selectivity and CO$_2$ selectivity for LPG synthesis

From n $=$ $\dfrac{Pv}{RT}$

Where   P   =   pressure (atm)

                 v   =   volume (L)

                 n   =   mole (mol)

                 R   =   82.057 atm·ml/mol·K

                 T   =   temperature (K)

Catalyst   mixed CZZA and Pd-ZSM-5/silica fibers

Weight of catalyst   1.0 g

Temperature   298 K

Pressure   1 atm

R constant   0.082 atm · L/mol · K

Flow rate input (V$_{in}$)   0.010 L/min

<u>mol input synthesis gas (n$_{in,syn\ gas}$)</u>

$$= \frac{1\ atm \times 0.010\ L/min}{0.082\ atm \cdot \dfrac{ml}{mol \cdot K} \times 298\ K}$$

= 0.000409   mol/min = 0.02454   mol/ h

W/F (g cat·h/mol)   = (1.0÷0.02454) = 40.7

Table A- 1 Area of synthesis gas before reaction

No.	Area			
	Ar	CO	CH$_4$	CO$_2$
1	2643.7	29934.0	-	4294.6
2	2613.4	29278.3	-	4504.2
3	2656.4	29517.9	-	4577.4
AVG	2637.8	29576.7	-	4458.7

Reactant	%concentration	mol%/unit area
CO	32	= 32 ÷ 29576.7 = 0.001082
CO$_2$	5	= 5 ÷ 4458.7 = 0.001121
Ar	3	= 3 ÷ 2637.8 = 0.00114

Table A- 2 Area of synthesis gas at 300 min of reaction

Area			
Ar	CO	CH$_4$	CO$_2$
4125.70	18848.86	-	8416.30

% CO conversion $= 100 \times [1 - (18848.86 \times 0.001082) \times (\dfrac{2637.8}{4125.70}) \div 32]$

$= \quad 59.3\%$

Table A- 3 Area of standard gas

STD	CH$_4$	C$_2$H$_4$	C$_3$H$_8$	C$_4$H$_{10}$	C$_5$H$_{12}$	C$_6$H$_{14}$
conc.	1	1	1	1	1	1
area	934423.6	17385155.7	26084551.8	33810741.6	30313992.9	4037903.8

Table A- 4 Measurement of area number of TCD performed with reaction temperature of 260 $^\circ$C, H$_2$/CO 2:1, W/F=40 g cat.h/mol with Si/Al ratio of 40, at 300 min

Time(min)	Area Number (TCD)			
	Ar	CO	CH4	CO2
30	3456.00	26247.50		9210.30
60	3658.20	25652.40		9044.30
90	3893.30	22561.20		8878.30
120	4035.80	21029.30		8712.30
150	4050.60	20148.20		8546.30
180	4060.50	19671.70		8380.30
210	4081.40	19573.70		8214.30
240	4094.90	19223.36		8048.30
270	4110.30	18936.11		8182.30
300	4125.70	18848.86		8416.30

Table A- 5 Measurement of area number of FID performed with reaction temperature of 260 $^\circ$C, H$_2$/CO 2:1, W/F=40 g cat.h/mol with Si/Al ratio of 40, at 300 min

Area Number (FID)								
CH4	C2H4	C2H6	C3H6	C3H8	C4-1	C4-2	C5	C6
254704.20		122132.50		686709.50	1881080.70	75788.60	114091.50	424518.30
289617.20		246252.70		517165.20	1740629.90	79593.20	114745.20	381734.70
497789.30		355831.10		1208401.20	1256733.10	165096.10	132829.70	226370.30
570889.20		449390.90		1563307.80	1829630.60	243897.70	199220.70	159851.20
509870.00		476058.80		1689402.60	2165916.00	290845.50	263308.90	227159.50
517736.30		484490.70		1814272.00	2254077.10	296817.30	310039.90	180788.70
521430.90		486321.40		1998722.10	2315760.00	300034.10	314849.10	191413.10
627906.63		492552.90		2013451.73	2395095.03	305087.57	319658.30	202037.50
233687.08		497684.20		2198111.48	2570017.30	309681.87	314467.50	212661.90
339467.50		552815.50		2252771.23	2744939.00	404276.17	319276.70	153286.30

From $\qquad$ n $\quad = \quad \dfrac{Pv}{RT}$

Where $\qquad$ P $\quad = \quad$ pressure (atm)

$\qquad\qquad$ v $\quad = \quad$ volume (L)

$\qquad\qquad$ n $\quad = \quad$ mole (mol)

$\qquad\qquad$ T $\quad = \quad$ temperature (K)

$\qquad\qquad$ R $\quad = \quad$ 82.057 atm·ml/mol·K

mol C_1 $\quad = \quad$ [(339467.5÷934423.6)✕30✕10✕1.0÷100] ÷22400

$\qquad\qquad = \quad$ 4.866×10^{-5} mol/min

mol C_2 $\quad = \quad$ [(552815.5÷17385155.7)✕30✕10✕1.0÷100] ÷22400

$\qquad\qquad = \quad$ 4.26×10^{-6} mol/min

mol C_3 $\quad = \quad$ [(2252771.23÷26084551.8)✕30✕10✕1.0÷100] ÷22400

$\qquad\qquad = \quad$ 1.157×10^{-5} mol/min

mol C_4 $\quad = \quad$ [(2744939.0÷33810741.6)✕30✕10✕1.0÷100]÷22400

$\qquad\qquad = \quad$ 1.087×10^{-5} mol/min

mol C_5 $\quad = \quad$ [(319276.7÷30313992.9)✕30✕10✕1.0÷100] ÷22400

$\qquad\qquad = \quad$ 1.41×10^{-6} mol/min

mol C_6 $\quad = \quad$ [(153286.3÷4037904)✕30✕10✕1.0÷100] ÷22400

$\qquad\qquad = \quad$ 5.08×10^{-6} mol/min

mol total product $\quad = $ mol C_1+ mol C_2 +mol C_3 + mol C_4 +mol C_5+ mol C_6

$\qquad\qquad = \quad$ 8.185×10^{-5}

Hydrocarbon distribution/C%

C_1 $\qquad = \qquad$ $100 \times (339467.5 \div \sum total\ area\ C1\ to\ C6)$

$\qquad\qquad = \qquad$ 5.0

C_2 $\qquad = \qquad$ $100 \times (552815.5 \div \sum total\ area\ C1\ to\ C6)$

$\qquad\qquad = \qquad$ 8.4

C_3 $\qquad = \qquad$ $100 \times (2252771.23 \div \sum total\ area\ C1\ to\ C6)$

	=	34.1
C_4	=	$100\times(3149215\div\sum total\ area\ C1\ to\ C6)$
	=	47.6
C_5	=	$100\times(319276.70\div\sum total\ area\ C1\ to\ C6)$
	=	4.8
C_6	=	$100\times(153286.30\div\sum total\ area\ C1\ to\ C6)$
	=	2.3

$\therefore$ CO$_2$ Selectivity $\quad=\quad 10000\times[(8416.3\times0.00108\times0.986)\times(\dfrac{2637.8}{4125.70})\text{-}5]$

$\div(59.3\times32) \qquad = \qquad 3.91\ \%$

$\therefore$ Hydrocarbon Selectivity $\quad=100\text{-}3.91 \qquad=96.09\%$

$\therefore$ LPG Selectivity $\qquad=\qquad 96.09\times[(34.1+47.6]\div100$

$\qquad\qquad\qquad\qquad\quad = \qquad 78.5\ \%$

Appendix B
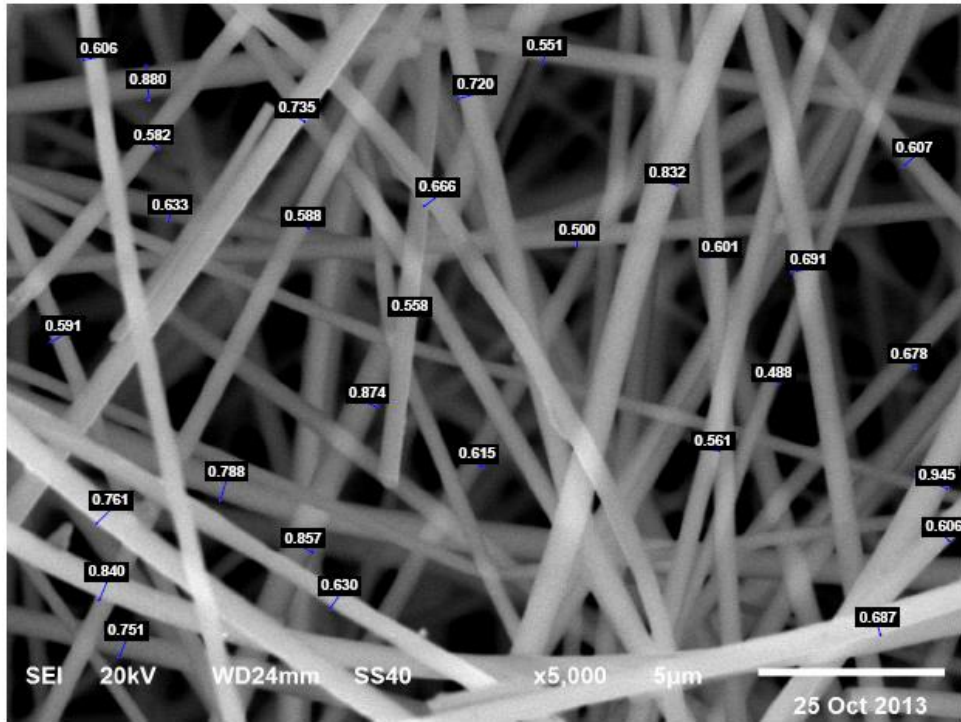
Figure B-1 Diameter of silica fibers measuring by SemAfore program
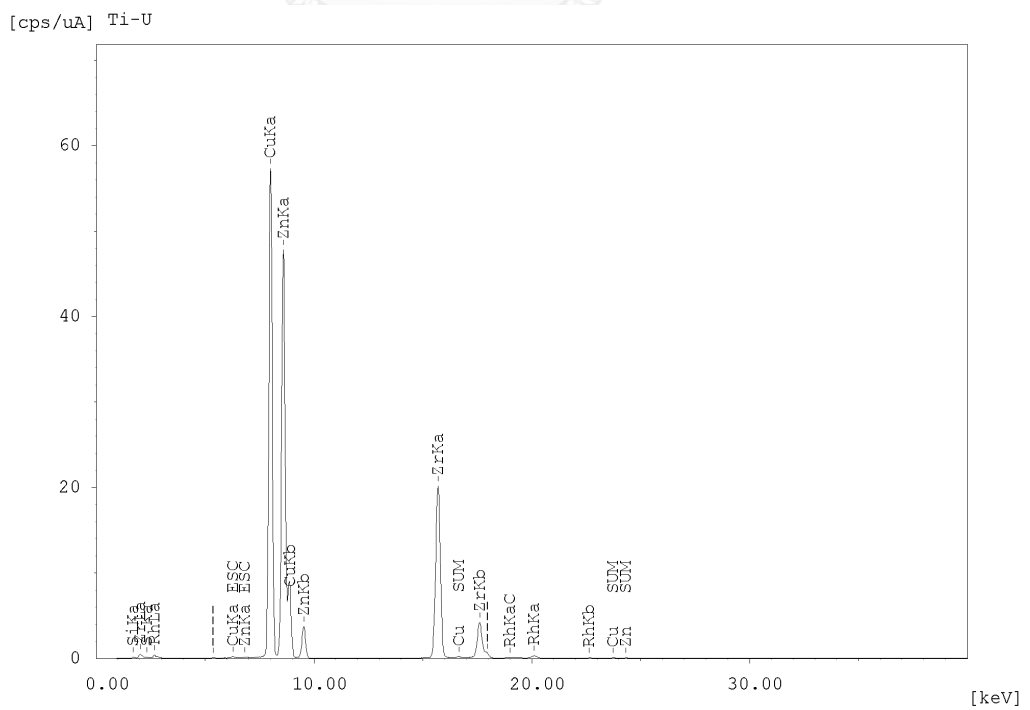
Figure B-2 The component of CZZA catalyst measured by EDX
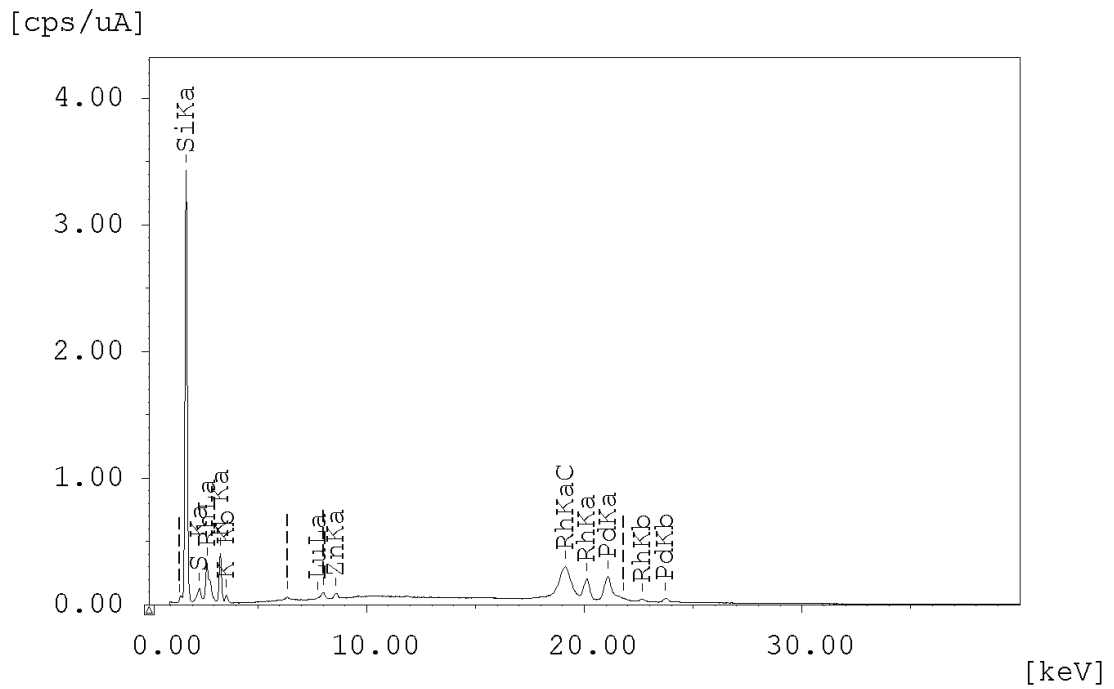
Figure B-3 The component of Pd-ZSM-5/silica fibers measured by EDX
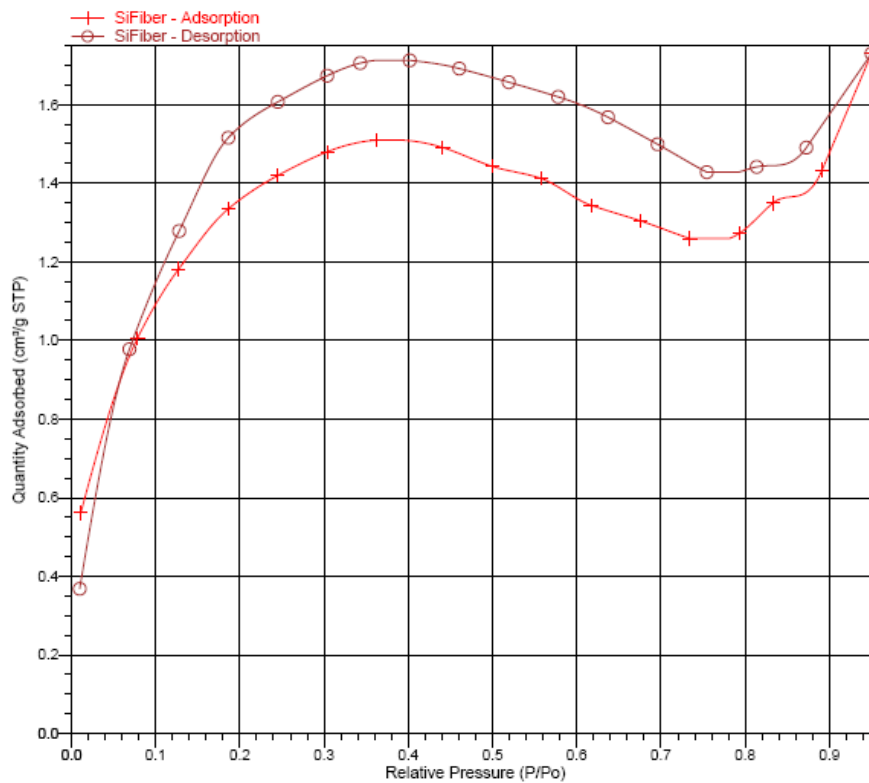
Figure B-4 N$_2$ physisorption of silica fibers

27Al exp. ZSM-5/ Silica fiber, use Al(NO3)3.9H2O as external std.(0 ppm).
spin 10000Hz.

Figure B-5 ^{27}Al-NMR of ZSM-5/silica fibers

VITA

Mr. Wittawat Ratanathavorn was born on December 13, 1984 in Bangkok, Thailand. He graduated from Chulalongkorn University in 2010 and holds a Master's degree of Science, major in Chemical Technology. After that he worked at Suan Dusit University as a lecturer during 2010-2012. Then, he has been studied the Doctoral's degree in Department of Chemical Technology, Chulalongkron University, Bangkok, Thailand since 2012 and finished his study in 2015. During 3 years of studied, he attended the oral presentation in The 4th Asian Conference on Innovative Energy & Environmental Chemical Engineering, Yeosu, South Korea on 9-12 December, 2014. Presented in the topic of "Synthesis of ZSM-5/silica fibrous catalyst by hydrothermal method"